cmgh
CELLULAR AND MOLECULAR GASTROENTEROLOGY AND HEPATOLOGY

ORIGINAL RESEARCH

Aspirin Rescues Wnt-Driven Stem-like Phenotype in Human Intestinal Organoids and Increases the Wnt Antagonist Dickkopf-1

Karen Dunbar,[1,2,3,a] Asta Valanciute,[1,3,a] Ana Cristina Silva Lima,[1,3] Paz Freile Vinuela,[1,2,3] Thomas Jamieson,[4] Vidya Rajasekaran,[1,2,3] James Blackmur,[1,2,3] Anna-Maria Ochocka-Fox,[1,2,3] Alice Guazzelli,[1,3] Patrizia Cammareri,[1,3] Mark J. Arends,[1,3] Owen J. Sansom,[4,5] Kevin B. Myant,[1,3] Susan M. Farrington,[1,2,3] Malcolm G. Dunlop,[1,2,3] and Farhat V. N. Din[1,2,3]

[1]Cancer Research UK Edinburgh Centre, MRC Institute of Genetics & Molecular Medicine, University of Edinburgh, Western General Hospital, Edinburgh; [2]MRC Human Genetics Unit, MRC Institute of Genetics & Molecular Medicine, University of Edinburgh, Western General Hospital, Edinburgh; [3]Institute of Genetics and Molecular Medicine, University of Edinburgh, Western General Hospital, Edinburgh; [4]Cancer Research UK Beatson Institute, Glasgow; and [5]Institute of Cancer Sciences, University of Glasgow, Glasgow, United Kingdom

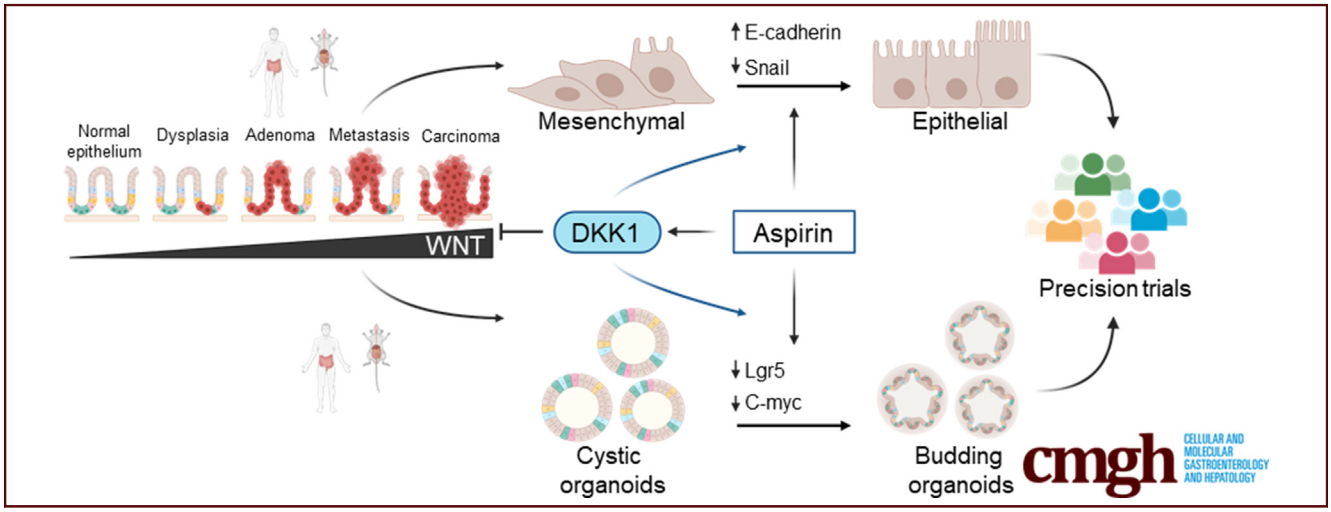

SUMMARY

Aspirin can reverse the Wnt-driven cystic phenotype in human organoids while reducing stem cell marker expression and increasing expression of Dickkopf-1, a Wnt antagonist often lost during CRC progression.

BACKGROUND & AIMS: Aspirin reduces colorectal cancer (CRC) incidence and mortality. Understanding the biology responsible for this protective effect is key to developing biomarker-led approaches for rational clinical use. Wnt signaling drives CRC development from initiation to progression through regulation of epithelial-mesenchymal transition (EMT) and cancer stem cell populations. Here, we investigated whether aspirin can rescue these proinvasive phenotypes associated with CRC progression in Wnt-driven human and mouse intestinal organoids.

METHODS: We evaluated aspirin-mediated effects on phenotype and stem cell markers in intestinal organoids derived from mouse ($Apc^{Min/+}$ and $Apc^{flox/flox}$) and human familial adenomatous polyposis patients. CRC cell lines (HCT116 and Colo205) were used to study effects on motility, invasion, Wnt signaling, and EMT.

RESULTS: Aspirin rescues the Wnt-driven cystic organoid phenotype by promoting budding in mouse and human Apc deficient organoids, which is paralleled by decreased stem cell marker expression. Aspirin-mediated Wnt inhibition in $Apc^{Min/+}$ mice is associated with EMT inhibition and decreased cell migration, invasion, and motility in CRC cell lines. Chemical Wnt activation induces EMT and stem-like alterations in CRC cells, which are rescued by aspirin. Aspirin increases expression of the Wnt antagonist Dickkopf-1 in CRC cells and organoids derived from familial adenomatous polyposis patients, which contributes to EMT and cancer stem cell inhibition.

CONCLUSIONS: We provide evidence of phenotypic biomarkers of response to aspirin with an increased epithelial and reduced stem-like state mediated by an increase in Dickkopf-1. This highlights a novel mechanism of aspirin-mediated Wnt inhibition and potential phenotypic and molecular biomarkers for trials. *(Cell Mol Gastroenterol Hepatol 2021;11:465–489; https://doi.org/10.1016/j.jcmgh.2020.09.010)*

Keywords: Epithelial-Mesenchymal Transition; Stem Cells; Organoids; Migration; Invasion.

Colorectal cancer (CRC) is the third most common cancer and second cause of cancer death worldwide.[1] The marginal improvement in survival for advanced disease highlights the need to pursue complementary approaches to target aberrant signaling underlying CRC initiation and progression. Compelling data show that aspirin decreases CRC incidence by 40%–50% and further suggest that post-diagnosis ingestion may delay progression and improve survival.[2–4] Understanding the biology responsible for the protective effect is key to developing biomarker-led precision prevention strategies.

Canonical Wnt signaling is central to gastrointestinal homeostasis and maintenance of the intestinal stem cell niche.[5] Dysregulated Wnt signaling, primarily driven by adenomatous polyposis coli (APC) mutations, is fundamental to cancer initiation in both sporadic CRC and familial adenomatous polyposis (FAP). Activation by Wnt ligands protects cytoplasmic β-catenin from destruction, leading to its nuclear translocation and T-cell factor (TCF)/lymphoid enhancer factor–dependent Wnt target gene induction.[5] Wnt signaling also governs both normal and cancer stem cell (CSC) regulation.[6,7] CSCs may arise from cancer cell dedifferentiation or from normal colonic stem cell transformation through increased intrinsic tumorigenesis or in response to microenvironmental cues.[8] Promisingly, Apc restoration triggers differentiation and polyp regression and realigns crypt homeostasis, highlighting a dynamic process that may be exploited.[9] Normally, secretion of endogenous Wnt antagonists serves to curtail excessive Wnt signaling.[5] Whereas some secreted inhibitors that sequester Wnt ligands do not inhibit Wnt in APC mutant cells, Dickkopf-1 (DKK-1) does inhibit Wnt signaling either by disrupting the low-density lipoprotein receptor-related protein 6 (LRP6)-frizzled complex or by promoting inactive LRP6 receptor internalization.[10] Ectopic expression studies of DKK-1 have established its role in intestinal crypt regulation.[11–13] DKK-1 is down-regulated during adenoma to carcinoma development, with low expression correlating with increased tumorigenesis.[14] Furthermore, DKK-1 is decreased in Western diet fed Mlh1+/− mice, a Lynch syndrome model, because of increased promoter methylation highlighting it is an early event.[15]

In addition to direct intestinal stem cell regulation, increased Wnt remodels the tumor microenvironment to drive cancer progression through epithelial-mesenchymal transition (EMT).[16,17] Poor CRC survival is associated with increased EMT-inducing gene expression and mesenchymal histology.[18,19] Malignant cells co-opt EMT regulatory machinery to increase motility and metastatic properties through progressive loss of epithelial features, such as cell-cell junctions and polarity.[20] The plasticity of this process leads to hybrid phenotypes and mesenchymal-epithelial transition, which establishes metastases.[21] Furthermore, EMT induction by the transcription factors Snail, Slug, or Twist triggers a stem-like phenotype in several cancers.[8] It is likely the response to oncogenic signaling in CRC, through intrinsic cell-specific plasticity and microenvironment stimuli, determines the contribution of EMT to the acquisition of cancer stem properties.

Despite elevated Wnt being central to colorectal carcinogenesis, there are no inhibitors used clinically.[22] Challenges in inhibitor development, including the Wnt requirement for homeostasis and cross-regulating networks, drive the search for "druggable vulnerabilities."[22] Segregation of CRCs by Wnt ligand dependency may identify a subgroup suitable for small molecule inhibition, but the majority of CRCs are ligand-independent through intracellular Wnt component mutation.[8] Nonetheless, blocking Wnt-receptor activity in Apc null cells does inhibit Wnt signalling in a ligand-independent manner.[23] Hence, a drug such as aspirin, which targets several nodes within Wnt signaling or multiple pathways to combat redundancy, may be more effective.[24,25] Because of the limited clinical success of target-based drug discovery approaches, there is an accelerated drive toward disease-relevant phenotypic screening.[26] Several pathways dysregulated in CRC, including Wnt, converge to regulate both CSCs and EMT, highlighting pro-neoplastic phenotypes that themselves may serve as response biomarkers. Here we investigate the inhibitory effect of aspirin on pro-neoplastic CSC and EMT phenotypes in CRC animal and human FAP organoid models and whether these effects can be attributed to inhibition of canonical Wnt signaling.

Results

Aspirin Reverses the Wnt-Driven Cystic Organoid Phenotype

Intestinal organoids are an invaluable tool for studying stem cell biology and Wnt signaling in a 3-dimensional ex vivo model. Increasingly organoid morphology can be

[a]Authors share co-first authorship.

Abbreviations used in this paper: **APC, adenomatous polyposis coli; CRC, colorectal cancer; CSC, cancer stem cell; DKK-1, Dickkopf-1; EMT, epithelial-mesenchymal transition; F-actin, filamentous actin; FAP, familial adenomatous polyposis; GSK-3B, glycogen synthase kinase 3B; HRP, horseradish peroxidase; LGR5, leucine-rich repeat-containing G-protein coupled receptor 5; LRP6, low-density lipoprotein receptor-related protein 6; PBS, phosphate-buffered saline; RhoA, ras homolog gene family, member A; ROCK1, rho-associated protein kinase 1; ROCK2, rho-associated protein kinase 2; siRNA, small interfering RNA; TCF, T-cell factor; TROY, tumor necrosis factor receptor superfamily member 19; ZO-1, zona occludens 1.**

Most current article

2352-345X
https://doi.org/10.1016/j.jcmgh.2020.09.010

exploited to uncover Wnt signaling mechanisms.[27] Intestinal organoids are composed of the familiar budding projections representing crypt-like structures, crypts with the intervening cells mimicking villi.[28] The budding projections are initiated by an $Lgr5^{+}$ stem cell and maintained through microenvironment recapitulation by growth factors.[29] This characteristic budding morphology is driven by Wnt signaling during intestinal homeostasis.[28] Loss of the wild-type APC allele in the $Apc^{Min/+}$ model drives increasingly cyst-like organoids reflecting the growth advantage.[30] Excessive Wnt activation, via genetic silencing of APC or exogenous Wnt, promotes this cystic phenotype. Although the transcriptional response regulated by genetic inactivation of APC and exogenous Wnt3a differs, both result in cystic organoid morphology, highlighting the utility of this phenotype as Wnt activation readout irrespective of the underlying mechanism.[31,32] Local Wnt signaling, critical for normal stem cell function and bud formation, is dysregulated in $Apc^{Min/+}$, $Apc^{flox/flox}$, and FAP adenoma organoids that grow in a characteristic cystic manner without budding structures (Fig. 1*A*).[29] The selective advantage for cells that initiate cystic organoids over budding organoids provides a window to test preventive agents.[30] Because trials of aspirin show benefit in sporadic and familial adenoma patients, we investigated whether aspirin alters the Wnt-driven cystic phenotype in organoids. Exposing small intestinal organoids grown from an $Apc^{flox/flox}$ mouse to 2 mmol/L aspirin for 12 days increased the percentage of wild-type phenotype (non-cystic) organoids, identified as those budding or with ruffled edges, compared with the untreated population (Fig. 1*B*, Supplementary Videos 1a and 1b). We next translated these effects to human organoids from macroscopically normal (non-adenomatous) and adenomatous colon tissue from FAP patients. The presence of cystic organoids in the normal mucosa sample may relate to the germline mutation or the presence of microadenomas due to loss of both APC copies. Longer exposure to 0.5 mmol/L aspirin for 29 days increased the percentage of budding organoids in populations derived from both "normal" and adenomatous colonic mucosa from FAP patients (Fig. 2*A*). In addition, treatment of $Apc^{Min/+}$ mice with aspirin for 4 weeks in vivo produced organoids that grew with a budding phenotype, in the absence of aspirin, compared with untreated $Apc^{Min/+}$ intestinal organoids, which remained spherical (Fig. 2*B*). Hence, we present robust evidence that aspirin rescues the cystic phenotype characteristic of constitutively active Wnt signaling due to a mutant Apc background.

Aspirin Decreases Stem Cell Marker Expression and Reduces Wnt Signaling

The organoid models' results suggest that aspirin mediates phenotype rescue by modulating $Lgr5^{+}$ stem cell populations or Wnt signaling gradients required for efficient organoid budding.[33] *Lgr5*, a Wnt target gene and receptor for the Wnt agonist R-spondin, is the principal stem cell marker in intestinal tissue, but others, such as tumor necrosis factor receptor superfamily member 19 (*TROY*), are also validated intestinal stem cell markers.[34] Basal Lgr5 and TROY transcript expression are increased in $Apc^{flox/flox}$ organoids compared with wild-type organoids, illustrating the increased stem cell number in Apc mutant tissue, and aspirin treatment reduces transcript expression of both markers in $Apc^{flox/flox}$ organoids (Fig. 3*A*). Using RNAscope technology we show that aspirin treatment reduces the relative expression of Lgr5 and TROY RNA transcripts per organoid (Fig. 3*B*). In the 4-week treatment $Apc^{Min/+}$ model, crypts isolated from aspirin-treated mice also show a decrease in Lgr5 and TROY stem cell marker transcript expression compared with untreated mice (Fig. 3*C*). Furthermore, aspirin treatment significantly reduced Lgr5 transcript expression in colonic organoids derived from human patient models representing normal mucosa, sporadic CRC, and FAP CRC (Fig. 3*D*). In FAP human organoids from normal and adenomatous tissue Lgr5 protein expression was also decreased with aspirin (Fig. 3*E*). These findings were replicated in vivo, with the treatment of $Apc^{Min/+}$ mice with aspirin for 4 weeks reducing the number of Lgr5 RNA transcripts per adenoma (Fig. 4*A*). The aspirin-mediated decrease in stem cell marker expression raised the possibility of niche alterations, specifically in Paneth cells, which are adjacent to $Lgr5^{+}$ cells. Paneth cell loss is known to drive a reduction in $Lgr5^{+}$ stem cells, highlighting a lead role in intestinal homeostasis.[35] Strikingly, aspirin decreased Paneth cell number, as identified by lysozyme immunohistochemistry, in small intestinal adenomas from $Apc^{Min/+}$ mice (Fig. 4*B*).

Wnt is the predominant pathway responsible for stem cell niche maintenance.[33] Aspirin treatment caused a slight reduction in the total β-catenin protein expression in small intestinal adenomas from $Apc^{Min/+}$ mice (Fig. 5*A*). Furthermore, aspirin treatment reduced transcript levels of *Tcf7*, the gene encoding Tcf1 protein that is a β-catenin co-transcriptional regulator, in $Apc^{Min/+}$ crypts and $Apc^{flox/flox}$ organoids (Fig. 5*B*). Nuclear β-catenin binds to the TCF transcription factor family to initiate Wnt target gene transcription,[5] including several EMT genes. Interestingly, contrary to the expectation of EMT at advanced disease stages, increased vimentin and decreased E-cadherin are observed in adenomas from several Apc-driven mouse models.[36] Aspirin increased E-cadherin and reduced vimentin expression in small intestinal adenomas from $Apc^{Min/+}$ mice (Fig. 5*C* and *D*). These observations further support that aspirin promotes a more epithelial phenotype in vivo and contributes to EMT inhibition through aspirin-mediated Wnt inhibition.

Aspirin Inhibits Wnt and Epithelial-Mesenchymal Transition While Reducing Migration and Invasion of Colorectal Cancer Cells

These in vivo observations were confirmed in Colo205 cells, with aspirin reducing expression of both β-catenin and its targets c-myc and Lgr5, while increasing E-cadherin expression (Fig. 6*A*). Further experiments confirmed that aspirin increases both protein and transcript expression of the epithelial marker E-cadherin in HCT116 and Colo205 cells (Fig. 6*B* and *C*). Aspirin also increased expression of a

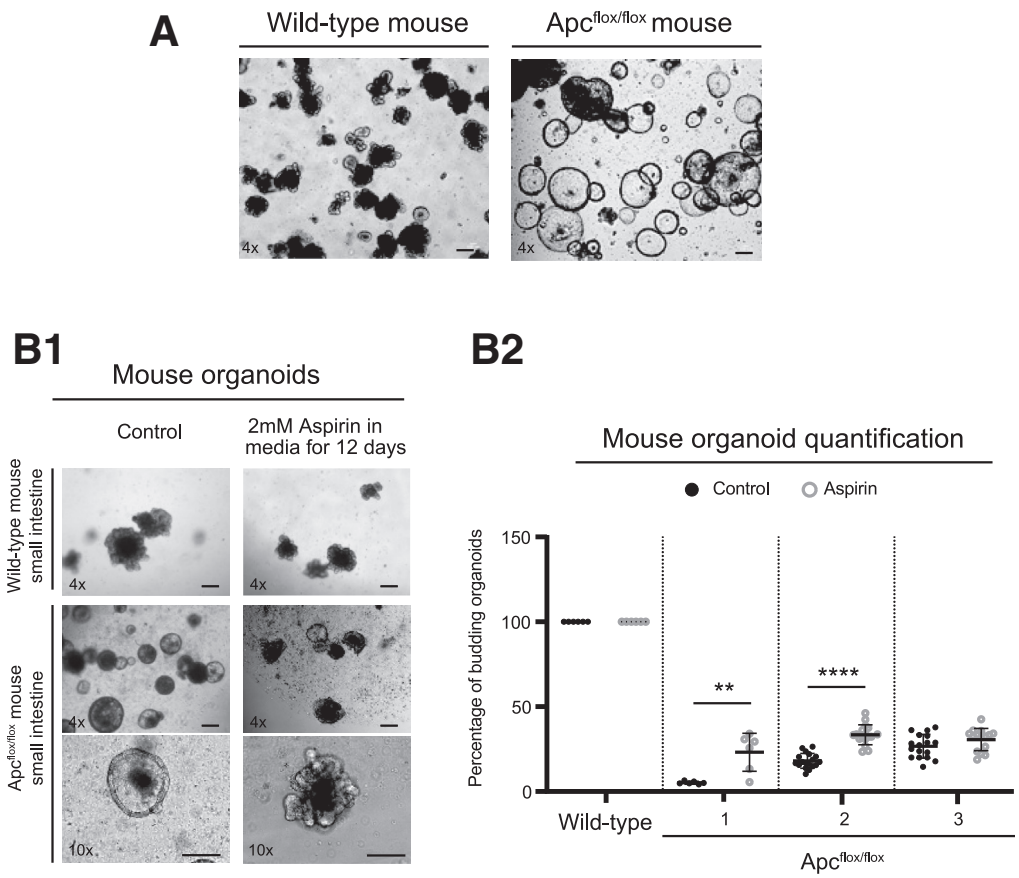

Figure 1. Aspirin reduces the Wnt-driven budding phenotype in mouse organoids. (*A*) Brightfield images of small intestinal organoids derived from wild-type (C57BL/6J) and $Apc^{flox/flox}$ mouse tissue. (*B1*) Brightfield images of small intestinal organoids derived from wild-type (C57BL/6j) and $Apc^{flox/flox}$ mouse tissue treated with 2 mmol/L aspirin for 12 days. (*B2*) Quantification of percentage of non-cystic organoids from 1 wild-type (C57BL/6J) mouse sample and 3 independent $Apc^{flox/flox}$ mouse samples treated with 2 mmol/L aspirin for 12 days. Microscope objective magnification noted in *bottom left corner* of image. Graphs represent individual data plots with overlay of mean and standard deviation. Statistical significance determined by Student *t* test. *Asterisks* denote *P* value (*<.05, **<.01, ***<.001, ****<.0001). Scale bar = 200 μm.

second epithelial marker, zona occludens 1 (ZO-1), but to a lesser extent than E-cadherin (Fig. 6*D*). Aspirin exposure reduced nuclear Snail protein expression, a key transcription factor that represses E-cadherin to drive EMT, while increasing cytoplasmic E-cadherin protein expression (Fig. 6*E*). These results indicate that aspirin is promoting an enhanced epithelial phenotype.

Increased migratory and invasive capabilities are characteristic of cells undergoing EMT and disease progression. Exposure to aspirin (0.5 and 3 mmol/L) reduced wound closure in HCT116 and Colo205 cells grown in both low (0.5%) and normal (10%) serum conditions (Fig. 7*A* and *B*). In low serum conditions cellular proliferation is inhibited; hence effects on wound closure more closely reflect alterations in migration rather than proliferation, thus increasing confidence that aspirin inhibits CRC cell migration. This is particularly important because aspirin has known antiproliferative effects especially at higher concentrations (Fig. 7*C*). Cellular invasion was modeled by using organotypic invasion assays using collagen-fibroblast matrices. Aspirin decreased both the distance invaded and the overall percentage of HCT116 and Colo205 cells invading, which was normalized to the noninvading population to remove any antiproliferative bias (Fig. 8*A* and *B*).

Consistent with inhibitory effects on invasion, aspirin exposure (0.5 and 3 mmol/L) reduced the distance single HCT116 and Colo205 cells travelled in 24 hours (Fig. 8*C* and *D*). Ras homolog gene family, member A (RhoA) signaling has been implicated in regulating CRC cell migration, invasion, and metastasis.[37] The effects of aspirin on RhoA signaling were focused on downstream effectors: rho-associated kinases 1 and 2 (ROCK1 and ROCK2), cofilin, and filamentous actin (F-actin).[38] Aspirin exposure reduced protein expression of the 2 kinases, ROCK1 and ROCK2 (Fig. 9*A*), and reduced levels of phosphorylated cofilin in both HCT116 and Colo205 cells (Fig. 9*B*). Switching the balance between phosphorylated and unphosphorylated cofilin alters F-actin stabilization and cycling, which drives cell movement.[39] Aspirin treatment reduced the overall F-actin expression, although no changes in F-actin stress fiber formation were observed (Fig. 9*C*). These results demonstrate that aspirin can inhibit several invasive traits commonly associated with EMT and disease progression.

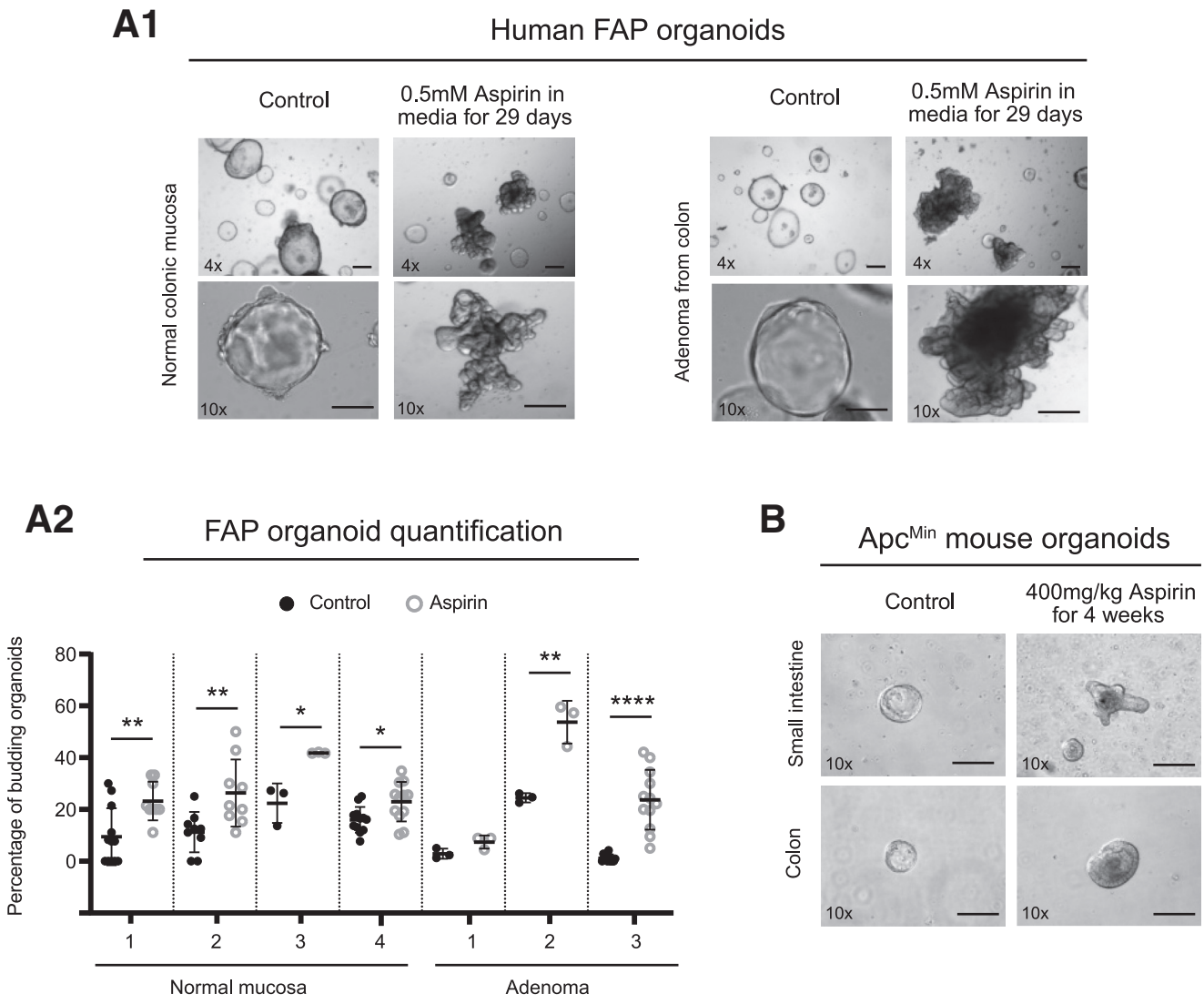

Figure 2. Aspirin reduces the Wnt-driven budding phenotype in human organoids. (*A1*) Brightfield images of organoids derived from human FAP normal colonic mucosa or adenomatous colon tissue treated with 0.5 mmol/L aspirin for 29 days. (*A2*) Quantification of percentage of budding organoids from 4 independent experiments of normal colonic mucosa derived organoids and 3 independent experiments of colonic adenoma derived organoids treated with 0.5 mmol/L aspirin for 29 days. (*B*) Brightfield images of small intestinal and colon organoids derived from control and aspirin-treated (400 mg/kg aspirin by oral gavage for 4 weeks) $Apc^{Min/+}$ mice. Microscope objective magnification noted in *bottom left corner* of image. Graphs represent individual data plots with overlay of mean and standard deviation. Statistical significance determined by Student *t* test. *Asterisks* denote *P* value (*<.05, **<.01, ***<.001, ****<.0001). Scale bar = 200 μm.

Aspirin Treatment Rescues Wnt-Driven Epithelial-Mesenchymal Transition and Stem Cell Changes in Colorectal Cancer Cells

We used the glycogen synthase kinase 3B (GSK-3β) inhibitor CHIR-99021 to hyperactivate Wnt signaling and investigate whether the aspirin-mediated inhibitory effects on EMT and stem cell markers are Wnt-regulated. Aspirin treatment abrogates CHIR-99021–mediated Wnt activation by increasing GSK-3β and β-catenin phosphorylation (Fig. 10*A*). The CHIR-99021–mediated increase in β-catenin and its targets, Axin2 and c-myc, are reversed on aspirin exposure (Fig. 10*B*). Wnt activation promotes a mesenchymal stem-like phenotype with decreased E-cadherin and increased Snail and Lgr5 expression, which was attenuated by aspirin in HCT116 cells (Fig. 10*C*). Increased E-cadherin has been shown to buffer excessive β-catenin, thus limiting hyperactivated Wnt and further promoting an epithelial phenotype.[40] Because of the increase in E-cadherin on aspirin treatment, we investigated the E-cadherin–β-catenin interaction. CHIR-99021 treatment led to a reduction in E-cadherin bound β-catenin that was rescued with aspirin treatment as demonstrated by co-immunoprecipitation experiments (Fig. 10*D*). The novel observation that the aspirin-mediated E-cadherin increase is paralleled by greater E-cadherin–β-catenin binding further supports the hypothesis that aspirin promotes an epithelial phenotype through Wnt inhibition.

The addition of CHIR-99021 to organoids grown from FAP normal tissue further promoted the cystic phenotype identified in Wnt hyperactive tissues, with all organoids appearing cystic after 15 days of treatment. This alteration in cystic: budding organoid ratio was rescued by exposure to aspirin (Fig. 10*E*). Furthermore, aspirin as a single agent

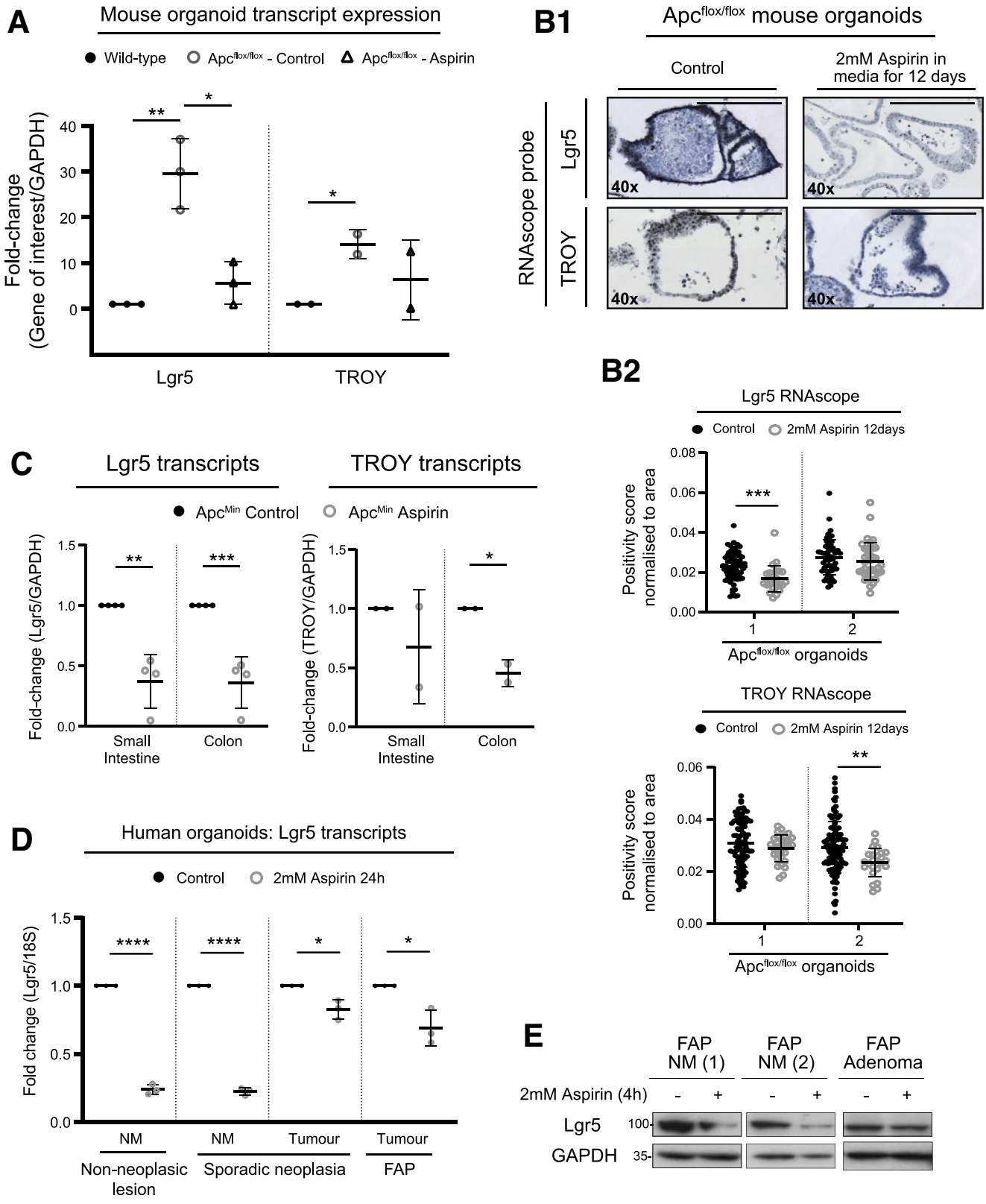

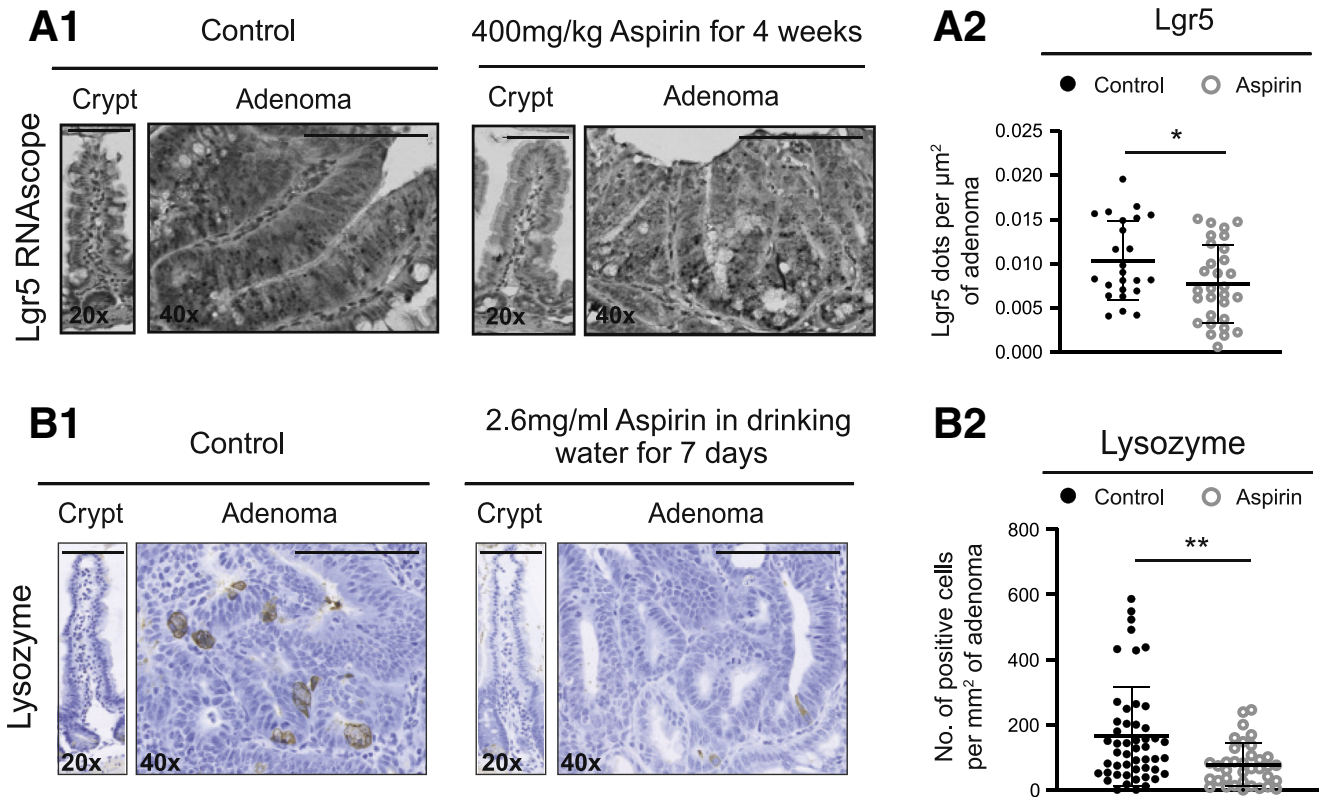

Figure 4. Aspirin reduces stem cell marker expression in vivo. (*A1*) Images of RNAscope staining for Lgr5 RNA expression in control and aspirin-treated (400 mg/kg aspirin by oral gavage for 4 weeks) $Apc^{Min/+}$ mouse tissue. (*A2*) Quantification of number of Lgr5 dots per μm^2 of adenoma tissue (24 control and 30 aspirin-treated adenomas) from cohort of 5 $Apc^{Min/+}$ control and 4 $Apc^{Min/+}$ aspirin-treated mice. (*B1*) Immunohistochemistry images of lysozyme expression in control and aspirin-treated (2.6 mg/mL aspirin in drinking water for 7 days) $Apc^{Min/+}$ mouse tissue. (*B2*) Quantification of lysozyme staining in adenoma tissue (50 control and 34 aspirin-treated adenomas) from cohort of 5 $Apc^{Min/+}$ control mice and 4 $Apc^{Min/+}$ aspirin-treated mice. Microscope objective magnification noted in *bottom left corner* of image. Graphs represent individual data plots with overlay of mean and standard deviation. Statistical significance determined by Student *t* test. *Asterisks* denote *P* value (*<.05, **<.01, ***<.001, ****<.0001). Scale bar = 50 μm.

or after CHIR-99021 reduced the expression of β-catenin and the stem cell markers, SOX9 and Lgr5 (Fig. 10*F*). Taken together, we show that aspirin treatment reverses the Wnt-driven EMT and stem phenotype in both CRC cell lines and organoids derived from human colonic mucosa from FAP patients.

Figure 3. (***See previous page***). **Aspirin reduces stem cell marker expression in organoids.** (*A*) Transcript expression of Lgr5 and TROY in untreated wild-type (C57BL/6J) mouse organoids and $Apc^{flox/flox}$ mouse organoids treated with 2 mmol/L aspirin for 12 days. Lgr5 and TROY transcript levels are normalized to GAPDH transcripts and expressed as fold-change compared with untreated control sample. Data represent 1 mouse per experimental condition. (*B1*) Images of organoids derived from $Apc^{flox/flox}$ mouse small intestine treated with 2 mmol/L aspirin for 12 days and stained with RNAscope probes for either Lgr5 or TROY. (*B2*) Quantification of organoids from 2 independent experiments (Lgr5-1, 54 control and 39 aspirin-treated organoids; Lgr5-2, 67 control and 25 aspirin-treated organoids; TROY-1, 92 control and 25 aspirin-treated organoids; TROY-2, 70 control and 31 aspirin-treated organoids). Quantification of RNAscope staining presented as a positivity score normalized to area. (*C*) Transcript expression of Lgr5 and TROY in isolated $Apc^{Min/+}$ mouse crypts treated with 400 mg/kg aspirin by oral gavage for 4 weeks. Lgr5 and TROY transcript levels are normalized to GAPDH transcripts and expressed as fold-change compared with untreated control sample. Data represent 1 control and 1 aspirin-treated $Apc^{Min/+}$ mouse. (*D*) Lgr5 transcript expression in organoids derived from human colonic tissue treated with 2 mmol/L aspirin for 24 hours. Lgr5 transcript levels are normalized to 18S transcripts, and data are expressed as fold-change compared with untreated control sample. Data represent organoids derived from 3 individual patients: a non-neoplastic lesion, sporadic neoplastic lesion, and adenoma tissue from a FAP patient. (*E*) Immunoblotting of Lgr5 protein abundance in organoids derived from human colonic tissue and treated with 2 mmol/L aspirin for 4 hours. Data from 3 individual human patient samples (2 normal colonic tissue samples and 1 colonic adenoma tissue sample). Microscope objective magnification noted in *bottom left corner* of image. Graphs represent individual data plots with overlay of mean and standard deviation. Statistical significance determined by Student *t* test. *Asterisks* denote *P* value (*<.05, **<.01, ***<.001, ****<.0001). Scale bar = 50 μm. NM, normal mucosa.

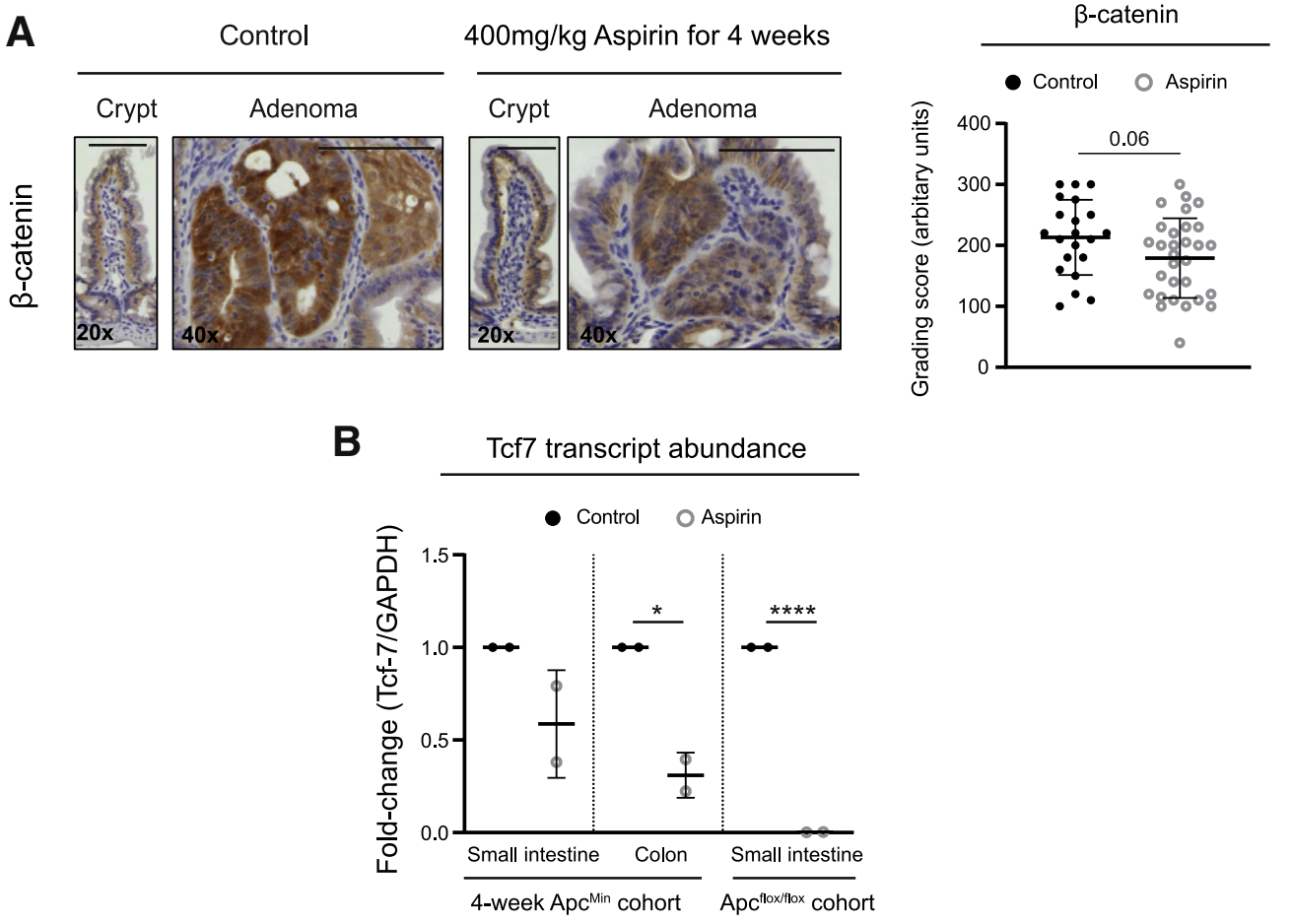
A
Control
400mg/kg Aspirin for 4 weeks
Crypt
Adenoma
Crypt
Adenoma
β-catenin
20x
40x
20x
40x
β-catenin
Control
Aspirin
Grading score (arbitary units)
400
300
200
100
0
0.06
B
Tcf7 transcript abundance
Control
Aspirin
Fold-change (Tcf-7/GAPDH)
1.5
1.0
0.5
0.0
*
****
Small intestine
Colon
Small intestine
4-week Apc^Min cohort
Apc^flox/flox cohort
C
Control
400mg/kg Aspirin for 4 weeks
Crypt
Adenoma
Crypt
Adenoma
E-cadherin
20x
40x
20x
40x
E-cadherin
Control
Aspirin
Grading score (arbitary units)
400
300
200
100
0
***
D
Control
400mg/kg Aspirin for 4 weeks
Crypt
Adenoma
Crypt
Adenoma
Vimentin
20x
40x
20x
40x
Vimentin
Control
Aspirin
No. of positive cells per mm² of adenoma
2000
1500
1000
500
0
**

Aspirin Increases Expression of the Wnt Inhibitor, Dickkopf-1

Studies reporting aspirin-induced Wnt inhibition have generally focused on destruction complex machinery and downstream gene effects. The loss of endogenous Wnt antagonists during colorectal carcinogenesis is well-recognized and may impact on survival. We focused on the Wnt inhibitor DKK-1 because it is a specific canonical Wnt antagonist. DKK-1 acts as a potent Wnt inhibitor by binding to the transmembrane receptor LRP6, thus preventing the LRP6-frizzled interaction and blocking canonical Wnt activation.[41] DKK-1 negatively correlates with EMT, and overexpression promotes an epithelial phenotype paralleled by decreased invasive capabilities of CRC cells.[42] Aspirin treatment markedly increases DKK-1 expression while decreasing LRP6 expression in CRC cells, and this is paralleled by a decrease in secreted DKK-1 in the media (Fig. 11*A* and *B*). The aspirin-mediated increase in DKK-1 is modestly attenuated, in relative terms, by CHIR-99021 because it decreases DKK-1 in untreated samples (Fig. 11*A* and *B*). Aspirin increases nuclear DKK-1 expression in HCT116 cells, which is associated with reduced nuclear c-myc and Snail protein expression (Fig. 11*C*). Aspirin treatment increased DKK-1 transcript expression in organoids from FAP patients' normal mucosa and adenoma tissue (Fig. 11*D*). Because DKK-1 expression can be silenced because of methylation, we used human fetal colonic organoids to minimize potential epigenetic effects in human adult colon. Aspirin treatment of fetal organoids significantly increased DKK-1 transcript expression (Fig. 11*E*), and although no alteration of the cystic phenotype was expected because of the shorter duration, there was a significant reduction in organoid size compared with controls (Fig. 11*F*). Using small interfering RNA (siRNA) to DKK1, we observe that siDKK-1 shows an increase in β-catenin and c-myc, a decrease in E-cadherin expression, and no change in Snail in untreated cells (Fig. 11*G*). Because the siRNA DKK-1 knockdown is incomplete, we observe partial abrogation of aspirin-mediated effects on EMT and stem markers. We observe that aspirin decreases stem function using clonogenicity assays with a reduction in $Apc^{flox/flox}$ organoid size and number at 7 and 14 days, respectively (Fig. 12*A* and *C*). Furthermore, we confirm that human recombinant DKK-1 similarly decreases $Apc^{flox/flox}$ organoid size and number (Fig. 12*D*–*F*). Overall, our data robustly show that aspirin increases DKK-1 expression in CRC cells and in FAP organoids, which is associated with decreased stem cell function.

Discussion

In addition to its CRC prevention role, aspirin may confer a survival benefit after cancer diagnosis. The challenge remains in delineating the dominant signaling pathways responsible and identifying biomarkers with clinical utility. Here, we show that aspirin rescues the Wnt-driven cystic organoid phenotype and reduces stem cell marker activity in colonic epithelium and adenomas from FAP patients. We also find that aspirin decreases the migratory and invasive capabilities of CRC cells while promoting an epithelial phenotype both in vitro and in mouse models. In exploring underlying mechanisms, we demonstrate for the first time that strikingly aspirin increases expression of the endogenous Wnt inhibitor, DKK-1, which contributes to the aspirin-mediated Wnt inhibition, decreases stem cell function, and enhances the epithelial phenotype.

The budding intestinal organoid phenotype recapitulates normal Wnt gradients during intestinal homeostasis.[27,43] We report the novel observation that aspirin rescues the characteristic aberrant Wnt-driven cystic phenotype by promoting budding in human normal mucosa and adenoma colonic organoids from FAP patients. This phenotype transition has been attributed to a concomitant decrease in proliferation and an increase in the elastic module that occurs during differentiation.[44] Cystic growth of intestinal organoids is further attributed to stem cell dysregulation due to hyperactivated Wnt. Both increased stem cell and mesenchymal marker expression are associated with poor CRC survival.[45,46] Reports suggest aspirin decreases stem cell markers in CRC cell lines.[47] Here, we establish in vivo relevance by using several Apc-driven mouse and human FAP organoid models to show that aspirin reduces both stem cell marker expression and function. Ectopic Paneth-like cells are observed in murine Apc-deficient colonic epithelium.[48] That aspirin decreases lysozyme expression, a Paneth cell marker, strongly suggests it also may be remodeling the stem cell niche generated by Paneth cell ligands and growth factors.[29] Interestingly, Paneth cell metaplasia, proposed as an early CRC marker, is observed

Figure 5. (*See previous page*). Aspirin reduces β-catenin and EMT markers in vivo. (*A*) Immunohistochemistry images and quantification of control and aspirin-treated (400 mg/kg aspirin by oral gavage for 4 weeks) $Apc^{Min/+}$ mouse tissue stained for β-catenin expression. (*B*) Transcript expression of Tcf7 in $Apc^{Min/+}$ mouse crypts treated with 400 mg/kg aspirin for 4 weeks and $Apc^{flox/flox}$ mouse organoids treated with 2 mmol/L aspirin for 12 days. Tcf7 transcript levels are normalized to GAPDH transcripts and expressed as fold-change compared with untreated control sample. Data represent 1 mouse per experimental condition. (*C*) Immunohistochemistry images and quantification of control and aspirin-treated (400 mg/kg aspirin by oral gavage for 4 weeks) $Apc^{Min/+}$ mouse tissue stained for E-cadherin expression. (*D*) Immunohistochemistry images and quantification of control and aspirin-treated (400 mg/kg aspirin by oral gavage for 4 weeks) $Apc^{Min/+}$ mouse tissue stained for vimentin expression. Quantification of β-catenin (21 control and 30 aspirin-treated adenomas), E-cadherin (37 control and 23 aspirin-treated adenomas), and vimentin (29 control and 16 aspirin-treated adenomas) staining in adenoma tissue from cohort of 5 $Apc^{Min/+}$ control and 4 $Apc^{Min/+}$ aspirin-treated mice. Microscope objective magnification noted in *bottom left corner* of image. Scale bar = 50 μm. Graphs represent individual data plots with overlay of mean and standard deviation. Statistical significance determined by unpaired Student *t* test. *Asterisks* denote *P* value (*<.05, **<.01, ***<.001, ****<.0001).

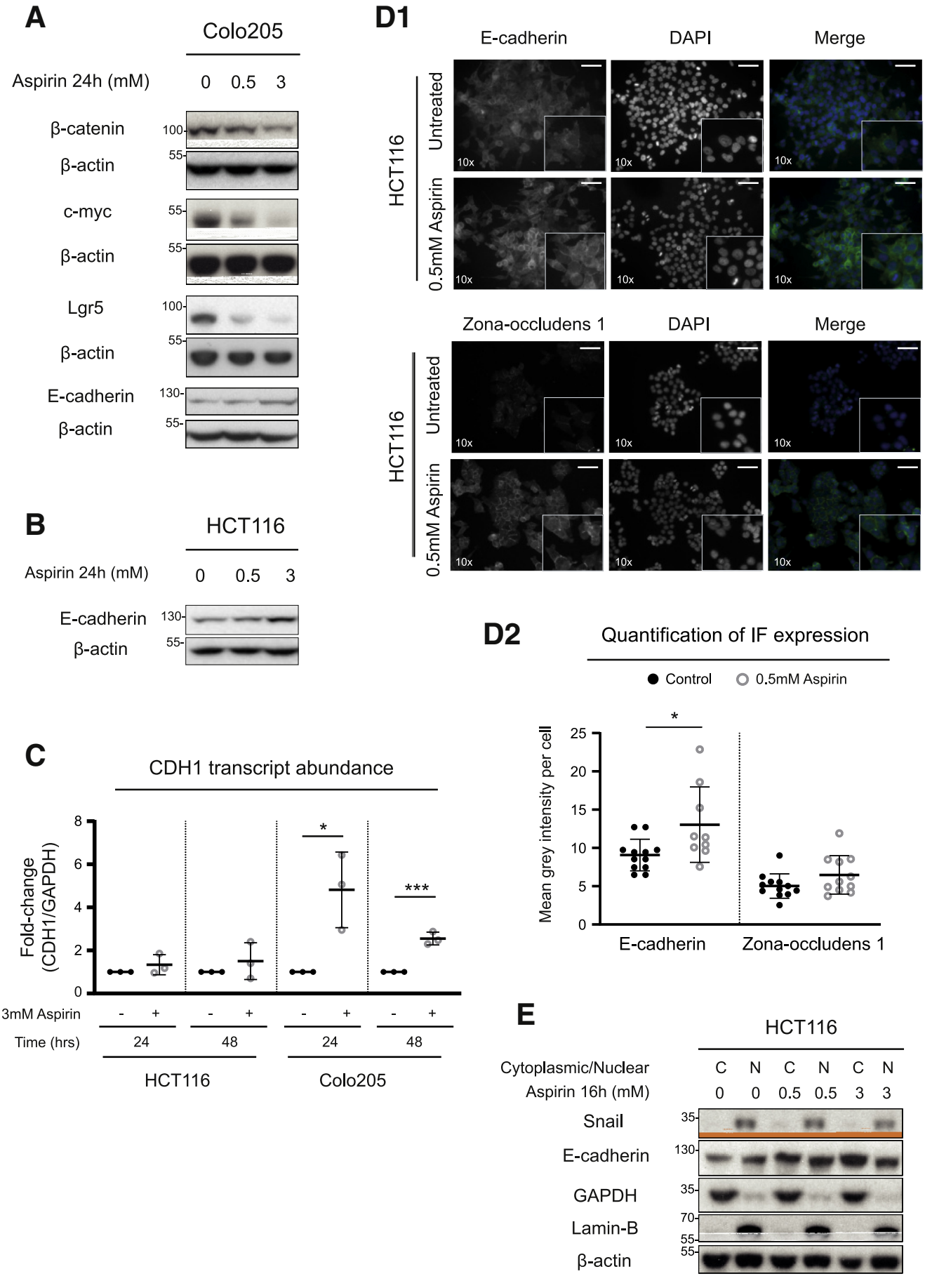
A
Colo205
Aspirin 24h (mM)
0 0.5 3
β-catenin
β-actin
c-myc
β-actin
Lgr5
β-actin
E-cadherin
β-actin
100
55
130
B
HCT116
Aspirin 24h (mM)
0 0.5 3
E-cadherin
β-actin
C
CDH1 transcript abundance
Fold-change (CDH1/GAPDH)
3mM Aspirin
Time (hrs)
24 48 24 48
HCT116
Colo205
D1
E-cadherin
DAPI
Merge
Zona-occludens 1
HCT116
Untreated
0.5mM Aspirin
10x
D2
Quantification of IF expression
Control
0.5mM Aspirin
Mean grey intensity per cell
E-cadherin
Zona-occludens 1
E
HCT116
Cytoplasmic/Nuclear
Aspirin 16h (mM)
C N C N C N
0 0 0.5 0.5 3 3
Snail
E-cadherin
GAPDH
Lamin-B
β-actin

less frequently in colonic mucosa of aspirin users.[49] Interestingly, detailed characterization of receptor-mediated signaling compared with APC loss suggests mutually exclusive gene signatures.[50] Our findings highlight 2 novel phenotypic indicators of aspirin response, the cystic-phenotype rescue and reduced stem cell marker expression, which may serve as enhanced biomarkers compared with individual Wnt components.

In addition to stem cell niche regulation, Wnt signaling drives EMT in collaboration with the master regulators transforming growth factor beta and mechanistic target of rapamycin. Further feedforward enhancement is highlighted as EMT and CSC induction increases Wnt activity and reduces DKK-1 expression in breast tissue.[51] Previous lung and CRC cell data suggest aspirin decreases migration through E-cadherin up-regulation via slug repression or by decreasing proinvasive metalloproteinases, respectively.[52,53] Indeed, supraphysiological aspirin attenuates CRC cell migration and platelet-mediated EMT.[54,55] Importantly, we show that aspirin-induced inhibition of migration and invasion and epithelial phenotype enhancement occur at physiologically relevant doses, independent of platelet inhibition in vitro. However, platelet and tumor cell interaction is context-dependent, and platelet inhibition may further contribute to the EMT-inhibitory effects of aspirin observed in the Apc mouse models.

Wnt activation using the GSK-3β inhibitor CHIR-99021 induces EMT and stem-like alterations in CRC cells, which are rescued by aspirin. The mechanistic basis of aspirin-induced Wnt inhibition is not established, and impact at both extrinsic and intrinsic Wnt nodes may strengthen efficacy.[56] Our results show that aspirin increases expression of DKK-1, an endogenous secreted Wnt antagonist that is down-regulated during CRC progression.[14] DKK-1 is a β-catenin/TCF4 target that attenuates canonical Wnt signaling.[57] This negative feedback is lost during CRC because of DKK-1 promoter hypermethylation, and demethylation restores DKK-1 expression and tumor suppression function.[58] Its role in intestinal homeostasis is further highlighted by knockdown leading to epithelial hyperproliferation in murine intestine.[59] Similar to the results shown here with aspirin, DKK-1 overexpression reduces cellular migration and invasion while promoting an epithelial phenotype and reduces stem cell marker expression, including Lgr5, in CRC cells.[42] In humans, high serum DKK-1 correlates with increasing CRC stage,[60] whereas tissue DKK-1 expression is lost with cancer progression. Here, we demonstrate that aspirin robustly increases DKK-1 expression in CRC models, which contributes to EMT and CSC inhibition observed with aspirin. Furthermore, there is a concomitant decrease in secreted DKK-1 levels, raising the possibility of using serum DKK-1 as a biomarker of response to aspirin. Interestingly, aspirin reduces plasma DKK-1 in type 2 diabetic patients, and exercise also reduces serum DKK-1 in breast cancer survivors, further highlighting its potential as a biomarker.[61,62]

Several potential mechanisms underlying the aspirin-mediated DKK-1 increase remain to be explored. Apc loss impairs DNA methylation to alter stem cell commitment to differentiation.[63] LSD1 is a highly expressed demethylase in CRC with knockdown leading to increased DKK-1 expression and decreased tumorigenic properties.[64] Aspirin also decreases methylation of promoter-associated CpGs in normal colon mucosa.[65] It is possible that aspirin increases DKK-1 expression through LSD1 inhibition, which demethylates DKK-1. Using mouse and human CRC models, our data identify novel phenotypic biomarkers of response to aspirin, with an increased epithelial and reduced stem-like state mediated by an increase in the Wnt antagonist DKK-1. Through targeting Wnt signaling at multiple levels, aspirin enhances commitment to differentiation, and hence phenotypic markers of Wnt inhibition represent better targets from therapeutic exploitation. Our observations reveal a novel mechanism of aspirin-mediated Wnt inhibition through DKK-1 increase and potential "pheno-markers" for chemoprevention and adjuvant aspirin human trials.

Materials and Methods

Animal Studies

All animal experiments were approved by either the University of Edinburgh or University of Glasgow ethics committee and performed under a UK Home Office project license. Tissues from 2 separate $Apc^{Min/+}$ mouse cohorts were analyzed in the production of this article. A 4-week treatment cohort consisted of 12 C57BL/6J mice and 12 $Apc^{Min/+}$ mice. Each group was separated into 6 aspirin-treated and 6 control mice. All treatment groups were composed of 3 male and 3 female mice except the C57BL/6J aspirin treatment group, which contained 1 male and 5 female mice. Treatment commenced at 6 weeks and lasted 4 weeks. Mice were administered distilled water or 400 mg/

Figure 6. (***See previous page***). **Aspirin reduces Wnt signaling and promotes an epithelial phenotype in CRC cells.** (*A*) Immunoblotting of β-catenin, c-myc, Lgr5, and E-cadherin protein abundance in Colo205 cells treated with 0.5 or 3 mmol/L aspirin for 24 hours. (*B*) Immunoblotting of E-cadherin protein expression in HCT116 cells treated with 0.5 or 3 mmol/L aspirin for 24 hours. (*C*) E-cadherin (CDH1) transcript expression in HCT116 and Colo205 cells treated with 3 mmol/L aspirin for either 24 or 48 hours. CDH1 transcript levels are normalized to GAPDH transcripts and expressed as fold-change compared with untreated control sample. Data represent 3 independent experiments. (*D1*) Immunofluorescence images of E-cadherin and zona occludens 1 staining in HCT116 cells treated with 0.5 mmol/L aspirin for 24 hours. (*D2*) Quantification of E-cadherin and zona occludens 1 staining in HCT116 cells treated with 0.5 mmol/L aspirin for 24 hours. Staining intensity quantified as mean grey intensity per cell. Data represent 2 independent experiments. (*E*) Immunoblotting of E-cadherin and Snail protein abundance in cytoplasmic/nuclear extracts from HCT116 cells treated with 0.5 or 3 mmol/L aspirin for 16 hours. Immunoblotting data representative of 3 independent experiments. Microscope objective magnification noted in *bottom left corner* of image. Scale bar = 50 μm. Graphs represent individual data plots with overlay of mean and standard deviation. Statistical significance determined by unpaired Student *t* test. *Asterisks* denote *P* value (*<.05, **<.01, ***<.001, ****<.0001).

kg aspirin by oral gavage daily. A 7-day treatment cohort consisted of 9 $Apc^{Min/+}$ mice, 4 aspirin-treated (1 male and 3 females) and 5 controls (5 females). Treatment commenced once symptoms of tumor burden, specifically pale feet, became apparent and continued for 7 days. Aspirin was administered via the drinking water at 2.6 mg/mL. Mice

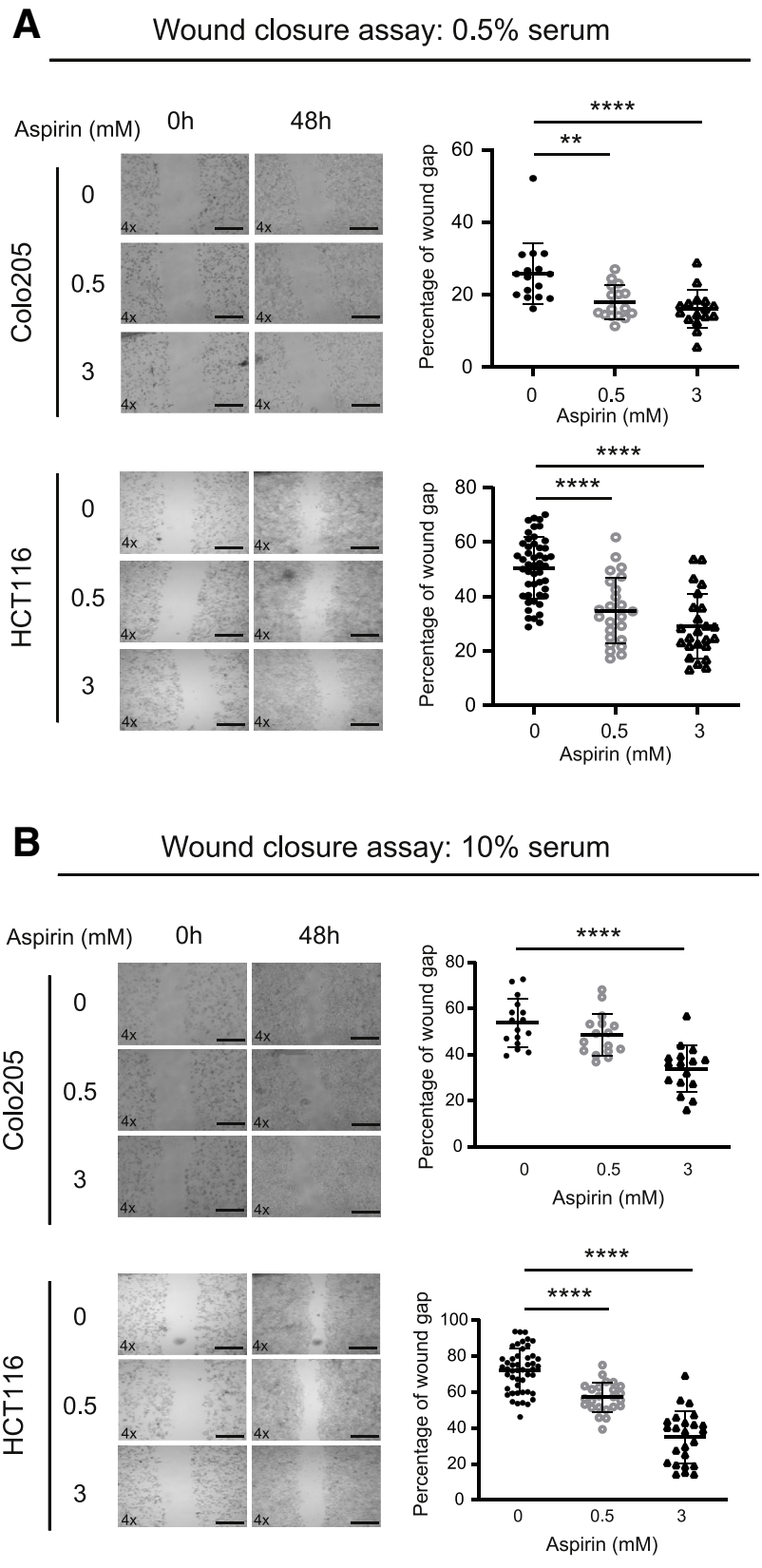

were culled after treatment by schedule 1 methods and tissue formalin-fixed and paraffin-embedded for histologic analysis.

Organoid Culture

The culture of colonic organoids from human tissue has been described previously.[29] Human colonic mucosa and adenomas were removed during surgery. After washing in phosphate-buffered saline (PBS), mucosa was incubated in crypt chelating solution (1× PBS, 45 mmol/L sucrose, 55 mmol/L D-sorbitol, 500 μmol/L DL-dithiothreitol, 5 mmol/L EDTA) for 1 hour at 4°C to dissociate the crypts. Crypts were dissociated from the mucosa by vigorous washing in PBS. Crypts were pelleted, washed, and embedded in BD Matrigel basement membrane matrix (BD Biosciences, San Jose, CA; 356234). Organoids were maintained in human colon mucosa medium (Advanced DMEM/F12 [Gibco, Waltham, MA; 12634028], 1× GlutaMax [Gibco, 35050038], 1 mol/L Hepes [Gibco, 15630106], 100 IU/mL penicillin and 100 μg/mL streptomycin [Lonza, Basel, Switzerland; 09-757F], 1× B27 [Gibco, 17504044], 1 mmol/L N-acetyl-L-cysteine [Sigma-Aldrich, St Louis, MO; A7250], 10 mmol/L nicotinamide [Sigma-Aldrich, 72340], 10 nmol/L gastrin [Sigma-Aldrich, G9020], 50 ng/mL epidermal growth factor [Sigma-Aldrich, E9644], 100 ng/mL mouse Noggin [Peprotech, Rocky Hill, NJ; 250-38], 500 ng/mL A83-01 [Sigma-Aldrich, SML0788], 10 μmol/L SB202190 [Sigma-Aldrich, S7067], 100 mmol/L prostaglandin E_2 [Sigma-Aldrich, P5640], 1 μg/mL human R-spondin 1 [R&D Systems, Minneapolis, MN; 4645-RS], and 100 ng/mL human Wnt-3a [R&D, 5036-WN]), which was replaced every 2–3 days with passage 1:4 every 5–7 days. Adenomas were incubated in digestion media (Advanced DMEM/F12 [Gibco, 12634028], 1× GlutaMax [Gibco, 35050038], 1 mol/L Hepes [Gibco, 15630106], 100 IU/mL penicillin and 100 μg/mL streptomycin [Lonza, 09-757F], 1 mg/mL collagenase [Sigma-Aldrich, SCR103], 1× Y27632 [Tocris, Bristol, UK; 1254], 20 ng/mL hyaluronidase [Sigma-Aldrich, H3506]) at 37°C for 1 hour. The solution was placed through 70-μm cell strainer to remove fibrous material, and cells were washed and embedded in BD Matrigel basement membrane matrix (BD Biosciences, 356234). Organoids were maintained in human colon adenoma medium without human Wnt-3a and with the addition of 1× Y27632 (Tocris, 1254), which was replaced every 2–3 days with passage 1:4 every 5–7 days.

Mouse small intestine was removed after culling by schedule 1 methods. The tissue was incubated in 3 mmol/L EDTA for 30 minutes at 4°C to dissociate crypts. Crypts were dissociated by vigorous washing in PBS. Crypts were pelleted, washed, and embedded in BD Matrigel basement membrane matrix (BD Biosciences, 356234). Organoids were maintained in mouse small intestine medium (Advanced DMEM/F12 [Gibco, 12634028], 1× GlutaMax [Gibco, 35050038], 1 mol/L Hepes [Gibco, 15630106], 100 IU/mL penicillin and 100 μg/mL streptomycin [Lonza, 09-757F], 1× B27 [Gibco, 17504044], 50 ng/mL epidermal growth factor [Sigma-Aldrich, E9644], 100 ng/mL mouse Noggin [Peprotech, 250-38], and 1 μg/mL mouse R-spondin 1 [R&D, 7150-RS]), which was replaced every 2–3 days with passage 1:4 every 5–7 days. Human fetal tissue was obtained with ethical approval (REC-08/S1101/11) from elective terminations between 12- to 16-week gestation. Fetal intestine was dissected and incubated in 2 mmol/L EDTA for 1 hour at 4°C to dissociate crypts. Crypts were mechanically dissociated by vigorous washing in PBS, pelleted, and embedded in BD Matrigel basement membrane matrix (BD Biosciences, 356234). Fetal organoids were maintained in human colon mucosa medium, which was replaced every 2–3 days with passage 1:4 every 5–7 days.

Live Cell Imaging

Images were acquired using 10× objective on a Zeiss Axio-Observer Z1 inverted microscope with ASI MS-2000 XY stage (Applied Scientific Instrumentation, Eugene, OR). Samples were illuminated using brightfield and acquired on a Retiga6000 CCD camera (Qimaging, Surrey, BC, Canada). Organoids were maintained at 37°C using a custom-made environmental enclosure (MRC Human Genetics Unit imaging facility). A 5% CO_2 atmosphere was maintained by an Okolabs chamber (Okolabs, Ottaviano, Italy). Images were captured every 1 hour for 48 hours, and videos were created using Image J software (https://imagej.nih.gov/ij/).

RNAscope

Organoids were mechanically removed from BD Matrigel basement membrane matrix using a p200 pipette to disrupt the Matrigel. Organoids were washed in PBS, pelleted, and fixed with 4% paraformaldehyde (Thermo Scientific, 28906) for 30 minutes at room temperature. After fixation, organoids were washed in PBS twice and then dehydrated by sequential incubations in 25%, 50%, and 70% ethanol for 15 minutes each. The organoid pellet was embedded in 4% agarose and then paraffin embedded. For RNAscope, 5-μm sections were cut from formalin-fixed paraffin-embedded blocks of organoids or mouse tissue.

RNAscope is commercially available from Advanced Cell Diagnostics (ACD, Newark, CA). Here, the probes used were mouse TROY (420241) and mouse Lgr5 (312171). Before

Figure 7. (***See previous page***). **Aspirin reduces cell migration in CRC cells.** (*A*) Brightfield images of wound closure assays and quantification of percentage of wound closure over 48 hours in Colo205 and HCT116 cells maintained in 0.5% serum. (*B*) Brightfield images of wound closure assays and quantification of percentage of wound closure over 48 hours in Colo205 and HCT116 cells maintained in 10% serum. Wound closure assay data representative of 3 independent experiments, each containing 3 technical replicates. Scale bar = 100 μm. (*C*) Growth curves of HCT116 and Colo205 cells treated with various concentrations of aspirin (0.1, 0.5, 1, 3, or 5 mmol/L) over 72 hours. Quantification presented as number of cells per mL. Data represent 3 independent experiments. *Error bars* represent the standard error. Graphs represent individual data plots with overlay of mean and standard deviation. Statistical significance determined by Student *t* test. *Asterisks* denote *P* value (*<.05, **<.01, ***<.001, ****<.0001).

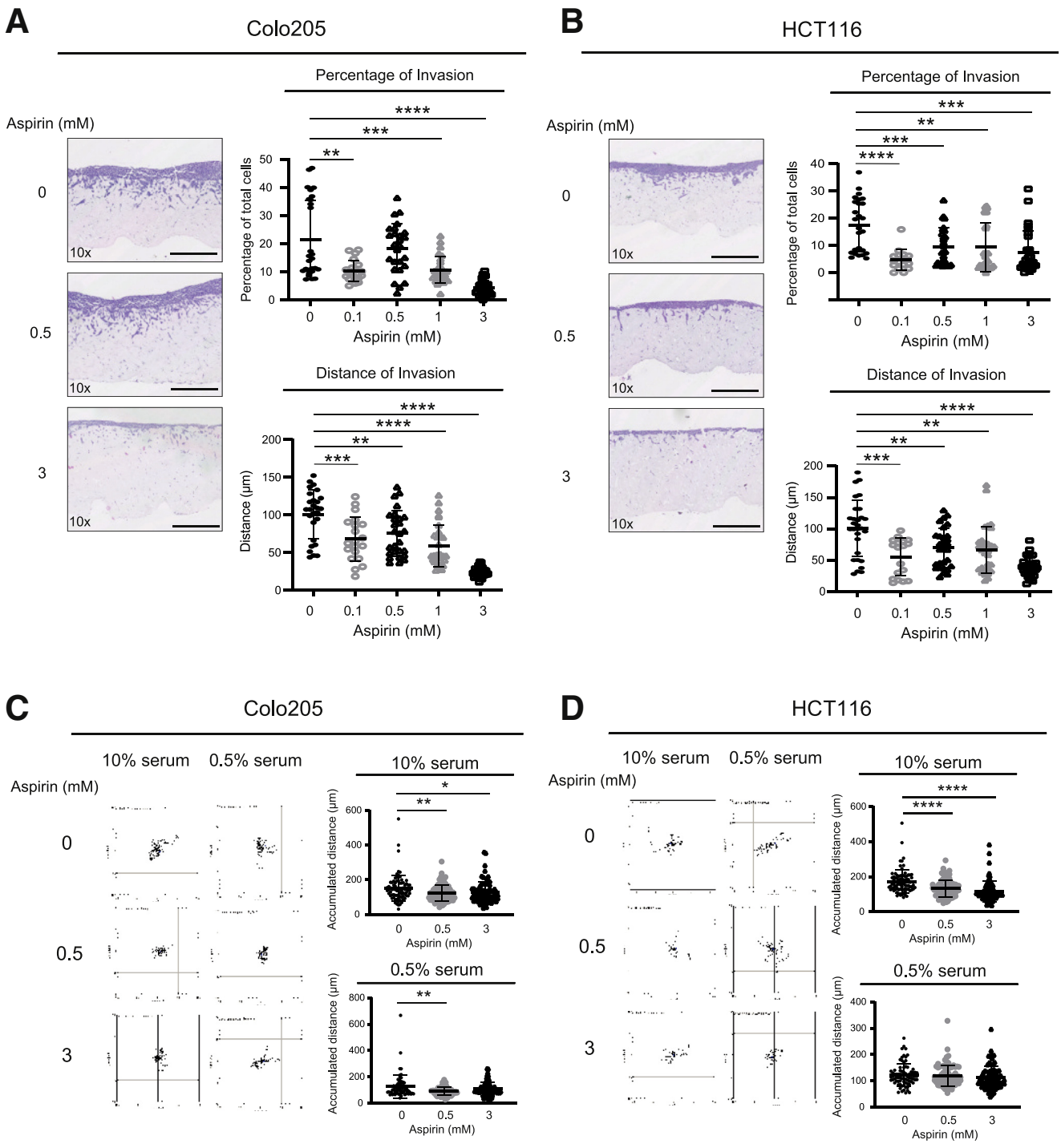

Figure 8. Aspirin reduces cell invasion and motility in CRC cells. (*A*) Brightfield images of hematoxylin-eosin stained organotypic invasion assays and quantification of percentage of cells invading and maximum distance invaded over 7 days with Colo205 cells. (*B*) Brightfield images of hematoxylin-eosin stained organotypic invasion assays and quantification of percentage of cells invading and maximum distance invaded over 7 days with HCT116 cells. Scale bar = 200 μm. Organotypic invasion assay data representative of 3 independent experiments, each containing 2 technical replicates. (*C*) Chemotaxis plots of cell movement and quantification of accumulated distance over 24 hours in Colo205 cells treated with 0.5 or 3 mmol/L aspirin and maintained in 0.5% or 10% serum. (*D*) Chemotaxis plots of cell movement and quantification of accumulated distance over 24 hours in HCT116 cells treated with 0.5or 3 mmol/L aspirin and maintained in 0.5% or 10% serum. Single cell motility data represent 3 independent experiments, each with 2 technical replicates. Microscope objective magnification noted in *bottom left corner* of image. Graphs represent individual data plots with overlay of mean and standard deviation. Statistical significance determined by Student *t* test. *Asterisks* denote *P* value (*<.05, **<.01, ***<.001, ****<.0001).

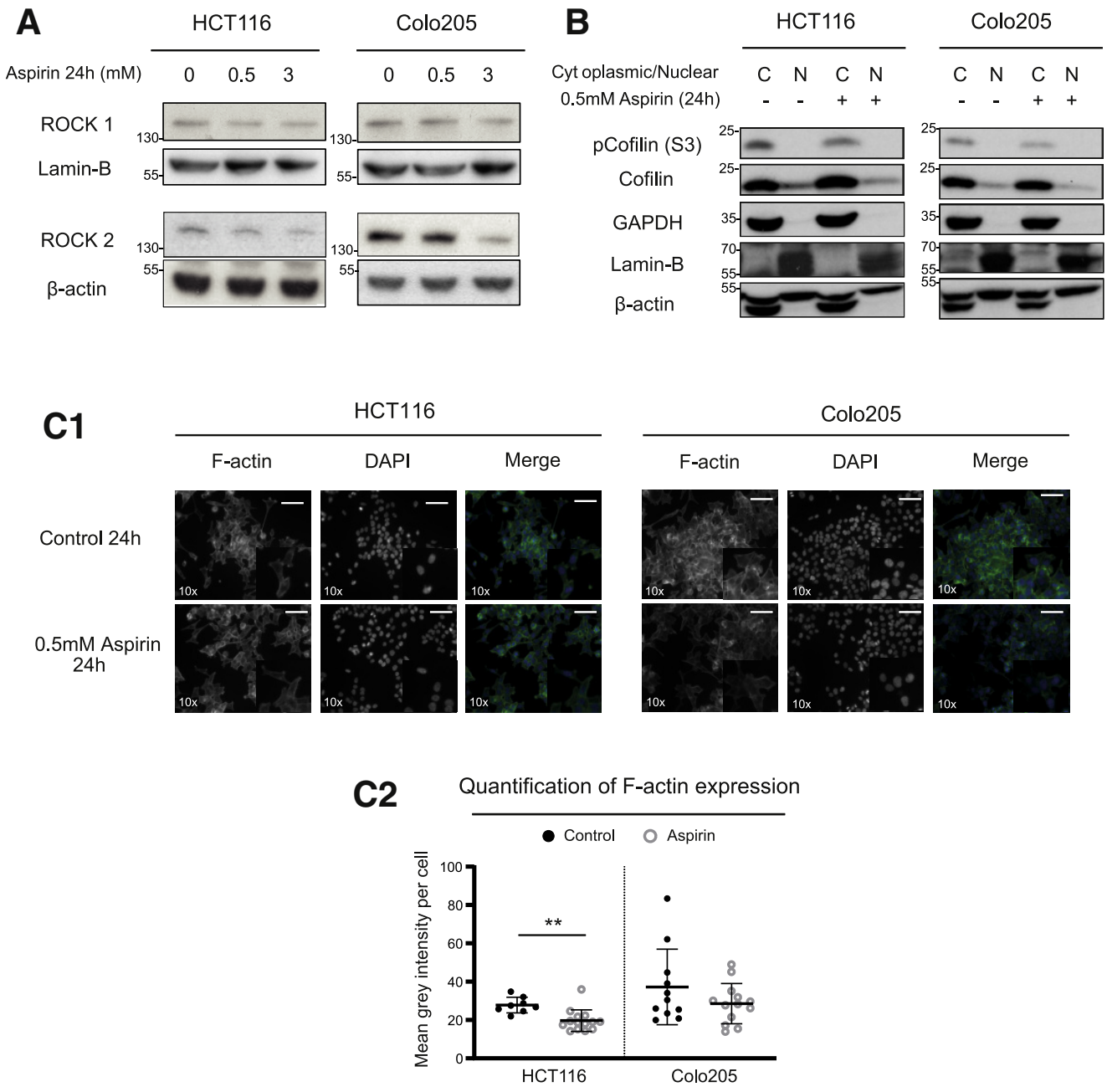

Figure 9. Aspirin reduces cell motility signaling pathway proteins. (*A*) Immunoblotting of ROCK 1 and ROCK 2 protein abundance in HCT116 and Colo205 cells treated with 0.5 or 3 mmol/L aspirin for 24 hours. (*B*) Immunoblotting of phosphocofilin (S3) and cofilin protein abundance in cytoplasmic/nuclear extracts treated with 0.5 mmol/L aspirin for 24 hours in HCT116 and Colo205 cells. Immunoblotting data representative of 3 independent experiments. (*C1*) Immunofluorescence images of F-actin staining in HCT116 and Colo205 cells treated with 0.5 mmol/L aspirin for 24 hours. (*C2*) Quantification of F-actin staining intensity in HCT116 and Colo205 cells treated with 0.5 mmol/L aspirin for 24 hours. Staining intensity quantified as mean grey intensity per cell. Data represent 2 independent experiments. Scale bar = 50 μm. Microscope objective magnification noted in *bottom left corner* of image. Graphs represent individual data plots with overlay of mean and standard deviation. Statistical significance determined by unpaired Student *t* test. *Asterisks* denote *P* value (*<.05, **<.01, ***<.001, ****<.0001).

treatment, target retrieval and peroxidase block of formalin-fixed paraffin-embedded sections were performed using RNAscope 2.5 HD Reagent kit-RED (ACD, 322350) according to manufacturer's instructions. After detection of the probes using 6 different amplification reagents, mRNA transcripts were visualized using diaminobenzidine substrate kit (Vector Laboratories, Burlingame, CA; SK-4100). Slides were counterstained with Gills hematoxylin (Sigma-Aldrich, GHS132). Slides were mounted using DPX mounting medium (Sigma-Aldrich,

1005790500), and slides were imaged using a NanoZoomer S60 digital slide scanner (Hamamatsu, Hamamatsu City, Japan). Quantification of RNAscope from adenoma tissue was completed manually using Image J software (https://imagej.nih.gov/ij/) to count all dots within an adenoma and normalized to the area. Quantification of RNAscope from organoids was completed using QuPath software.[66] All well-formed organoids present on the slide were analyzed by setting threshold values (for different intensities of diaminobenzidine staining to account for the number of amplification agents attach on the probes) and then calculating the number of positive cells.

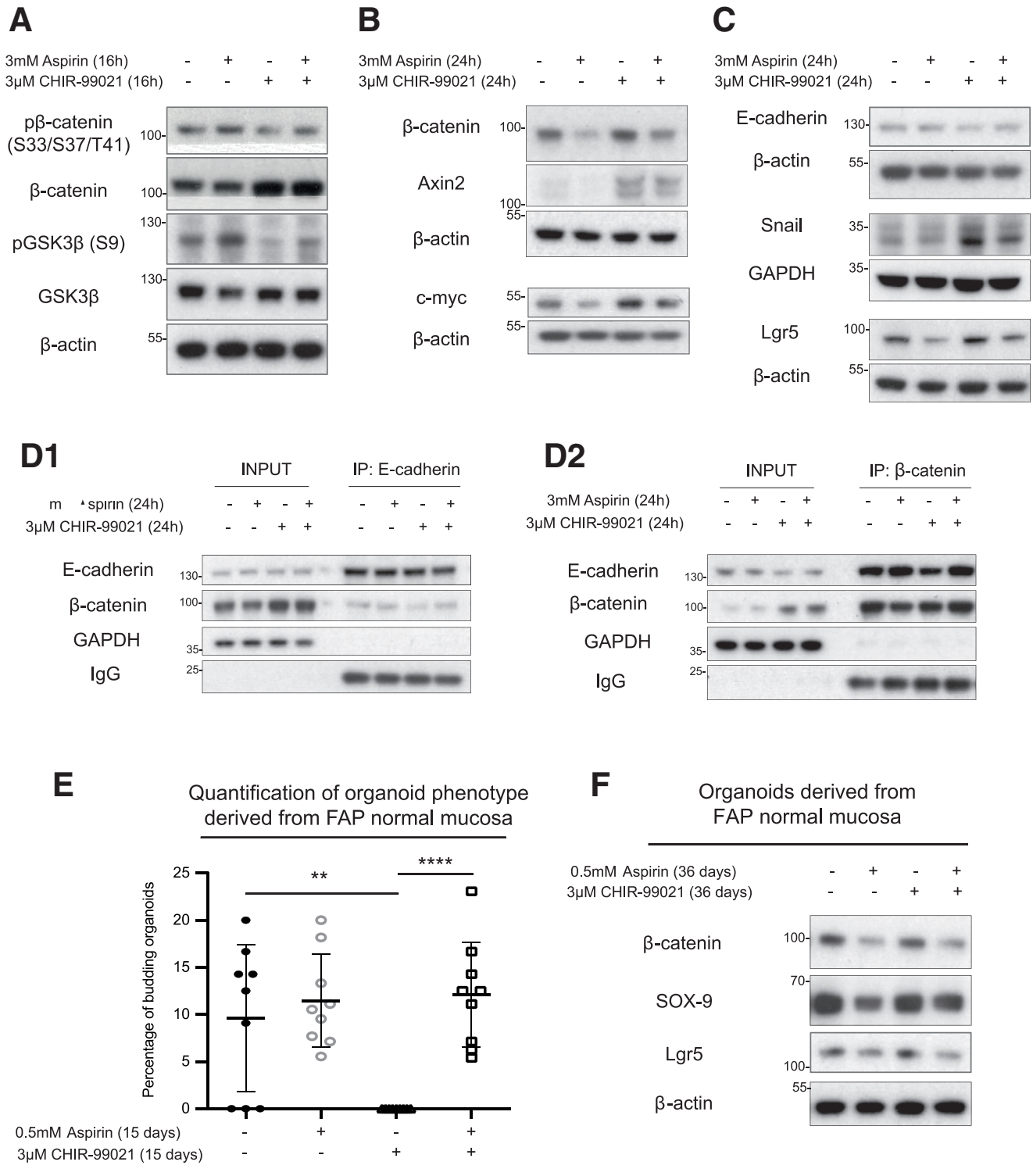

Immunohistochemistry

Formalin-fixed paraffin-embedded tissue blocks were cut into 5-μm-thick sections. Sections were deparaffinized by 3 × 5-minute washes in 100% xylene and sequentially washed in 3 × 100%, 1 × 90%, and 1 × 70% ethanol for 2 minutes each. Sections were incubated in water for 5 minutes to rehydrate. Antigen retrieval was completed by incubation in boiling 10% citrate buffer (Thermo Scientific, AP-9003). Endogenous blocking was achieved with incubation in 3% hydrogen peroxide (Sigma-Aldrich, H1009) for 10 minutes, followed by 5% goat serum (Thermo Scientific, 16210064) for 1 hour at room temperature. Primary antibody was diluted 1:200 in 5% goat serum (Thermo Scientific, 16210064) 0.01% Tween20 in PBS and incubated overnight at 4°C. After washing in 0.01% Tween20 in PBS, sections were incubated in EnVision horseradish peroxidase (HRP)–conjugated rabbit secondary antibody (Dako, Glostrup, Denmark; K400311-2) for 1 hour at room temperature. Sections were washed 3 × 10 minutes in 0.01% Tween20 in PBS. Signal was detected using diaminobenzidine substrate kit (Vector Laboratories, SK-4100). Sections were counterstained with Gills hematoxylin (Sigma-Aldrich, GHS132). Slides were mounted using DPX mounting medium (Sigma-Aldrich, 1005790500), and slides were imaged using a NanoZoomer S60 digital slide scanner (Hamamatsu). For quantification, an objective quantification method was used to avoid bias, and so all adenoma images were randomized, and quantification was completed blinded. The objective staining intensity number (0, negative; 1, mild; 2, moderate; 3, intense) was multiplied by the percentage of adenoma tissue expressing that intensity to give a grading score for each adenoma. For example, an adenoma with 50% mild staining and 50% moderate staining would be attributed a grading score of 150.

Cell Culture

CRC cell lines HCT116 (CCL-247) and Colo205 (CCL-222) are available from the American type culture collection (ATCC). HCT116 and Colo205 cells were grown as a monolayer in either McCoy's 5A Medium (Gibco, 16600082) or Dulbecco modified Eagle medium (Gibco, 41965039), respectively. Medium was supplemented with 10% fetal bovine serum (Hyclone, Logan, UT; 12379802), 100 IU/mL penicillin and 100 μg/mL streptomycin (Lonza, 09-757F). Cells were regularly tested for mycoplasma, with only mycoplasma free cell lines used for experimentation.

Antibodies

Antibodies recognizing E-cadherin (24E10) (3195), Snail (C15D3) (3879), ROCK1 (C8F7) (4035), ROCK2 (D1B1) (9029), cofilin (D3F9) (5175), phospho-cofilin (Ser3) (77G2) (3313), phospho-β-catenin (S33/37/41) (9561), phospho-GSK-3β (Ser9) (D85E12) (5558), GSK-3β (D5C5Z) (12456), Axin2 (76G6) (2151), Sox-9 (D8G8H) (82630) ZO-1 (D6L1E) (13663), and DKK-1 (D5V6L) (48367) were obtained from Cell Signaling Technology (Danvers, MA). Additional antibodies used were E-cadherin (BD Transduction Laboratories, 610181), β-catenin (BD Transduction Laboratories, 610153), c-myc (Abcam, Cambridge, United Kingdom; ab32072), GPCR GPR49 (Lgr5) (Abcam, ab75850), GAPDH (GeneTex, Irvine, CA; GTX627408), Lamin B (C-20) (Santa Cruz Biotechnology, Santa Cruz, CA; sc-6216), and β-actin (C4) (Santa Cruz Biotechnology, sc-47778). Secondary HRP-conjugated antibodies used were rabbit immunoglobulin G HRP-linked (GE Healthcare, Chicago, IL; GENA934) and mouse immunoglobulin G HRP-linked (GE Healthcare, GENA931).

Compound Treatments

Aspirin (Sigma-Aldrich, A2093) was added to cell culture medium at indicated concentrations (between 0.1 and 3 mmol/L) for the indicated duration. CHIR99021 (Tocris, 4423) is a GSK-3 inhibitor that was added to cells at a concentration of 3 μmol/L for 24 hours.

Wound Healing Assays

Cells were grown as a monolayer until 90% confluent, at which point a "wound" was created using a p200 pipette tip. Cells were washed in PBS twice to remove cellular debris before the addition of medium containing either 0.5% or 10% fetal bovine serum. Compound treatments were added as indicated, and brightfield images of the wound were taken at 0, 24, and 48 hours using a Zeiss Axiovert 100

Figure 10. (***See previous page***). **Aspirin reduces Wnt-driven mesenchymal and stem marker expression in CRC cell lines and FAP organoids.** (*A*) Immunoblotting of phospho-β-catenin (S33/S37/T41), β-catenin, phospho-GSK3β (S9), and GSK3β protein abundance in HCT116 cells treated with 3 mmol/L aspirin, 3 μmol/L CHIR-99021, or combination for 16 hours. (*B*) Immunoblotting of β-catenin, Axin2, and c-myc protein abundance in HCT116 cells treated with 3 mmol/L aspirin, 3 μmol/L CHIR-99021, or combination for 24 hours. (*C*) Immunoblotting of E-cadherin, Snail, and Lgr5 protein abundance in HCT116 cells treated with 3 mmol/L aspirin, 3 μmol/L CHIR-99021, or combination for 24 hours. Immunoblotting data representative of 3 independent experiments. (*D1*) Immunoprecipitation using E-cadherin antibody in HCT116 cells treated with 3 mmol/L aspirin, 3 μmol/L CHIR-99021, or combination for 24 hours and immunoblotting of β-catenin and E-cadherin from input lysates and immunoprecipitation elutes. (*D2*) Immunoprecipitation using β-catenin antibody in HCT116 cells treated with 3 mmol/L aspirin, 3 μmol/L CHIR-99021, or combination for 24 hours and immunoblotting of β-catenin and E-cadherin from input lysates and immunoprecipitation elutes. Immunoprecipitation data representative of 3 independent experiments. (*E*) Quantification of percentage of budding organoids derived from human FAP patient normal colonic mucosa tissue treated with 0.5 mmol/L aspirin, 3 μmol/L CHIR-99021, or combination for 15 days in vitro. Organoid data represent 1 individual human patient sample. (*F*) Immunoblotting of β-catenin, SOX-9, and Lgr5 protein abundance in organoids derived from human FAP patient normal colonic mucosa tissue treated with 0.5 mmol/L aspirin, 3 μmol/L CHIR-99021, or combination for 36 days in vitro. Organoid data represent 1 individual human patient sample. Graphs represent individual data plots with overlay of mean and standard deviation. Statistical significance determined by Student *t* test. *Asterisks* denote *P* value (*<.05, **<.01, ***<.001, ****<.0001).

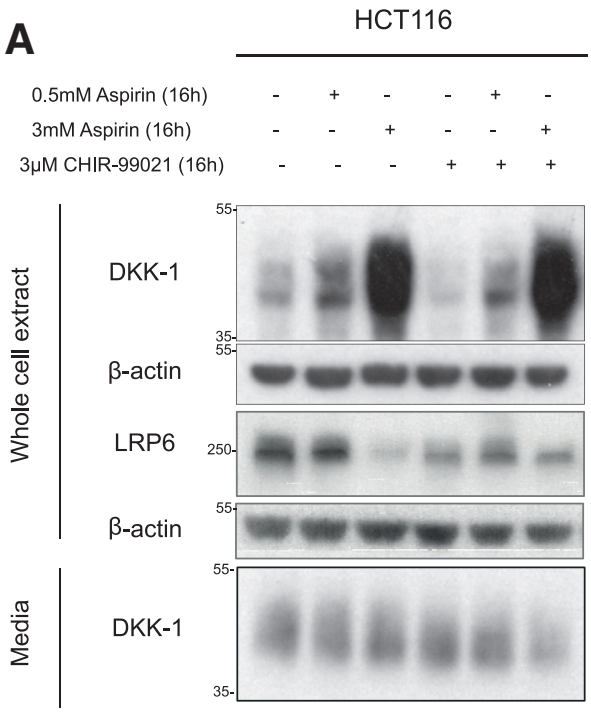
A
HCT116
0.5mM Aspirin (16h)
3mM Aspirin (16h)
3μM CHIR-99021 (16h)
Whole cell extract
DKK-1
β-actin
LRP6
β-actin
Media
DKK-1
55
35
250

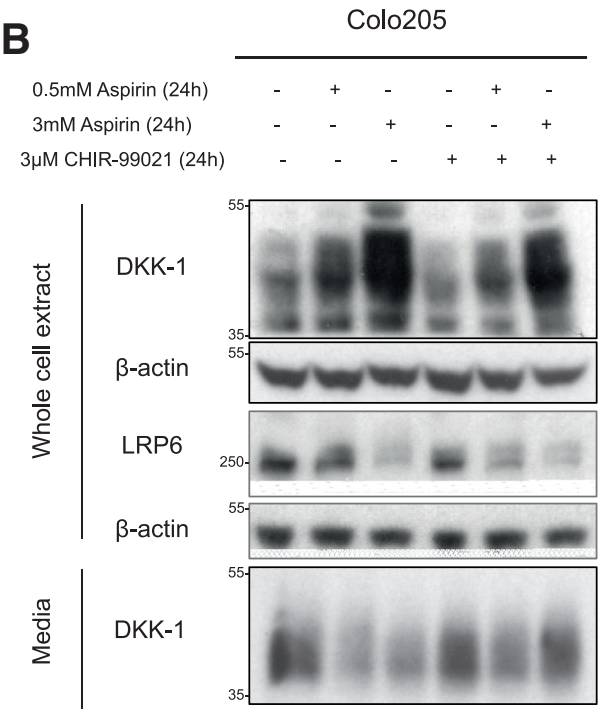
B
Colo205
0.5mM Aspirin (24h)
3mM Aspirin (24h)
3μM CHIR-99021 (24h)
Whole cell extract
DKK-1
β-actin
LRP6
β-actin
Media
DKK-1
55
35
250

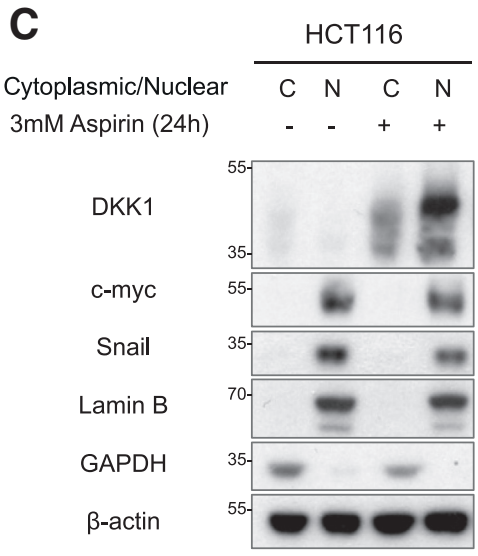
C
HCT116
Cytoplasmic/Nuclear
C N C N
3mM Aspirin (24h)
DKK1
c-myc
Snail
Lamin B
GAPDH
β-actin
55
35
70

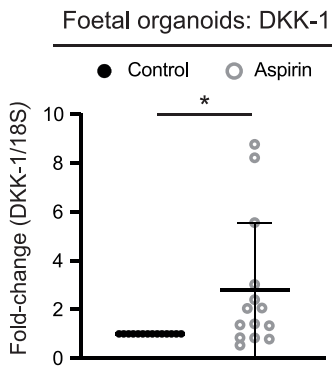
E
Foetal organoids: DKK-1
Control
Aspirin
*
Fold-change (DKK-1/18S)
0
2
4
6
8
10

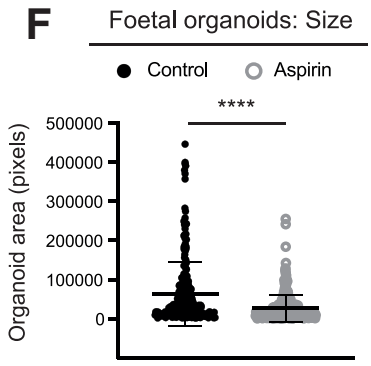
F
Foetal organoids: Size
Control
Aspirin
****
Organoid area (pixels)
0
100000
200000
300000
400000
500000

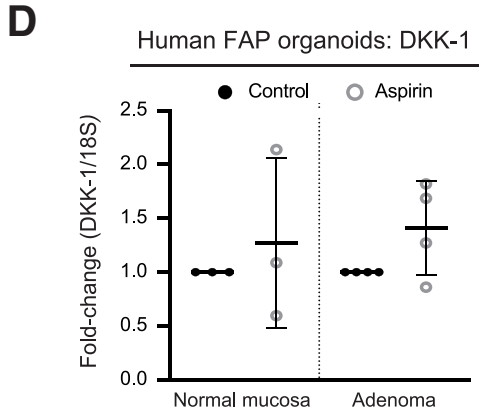
D
Human FAP organoids: DKK-1
Control
Aspirin
Fold-change (DKK-1/18S)
0.0
0.5
1.0
1.5
2.0
2.5
Normal mucosa
Adenoma

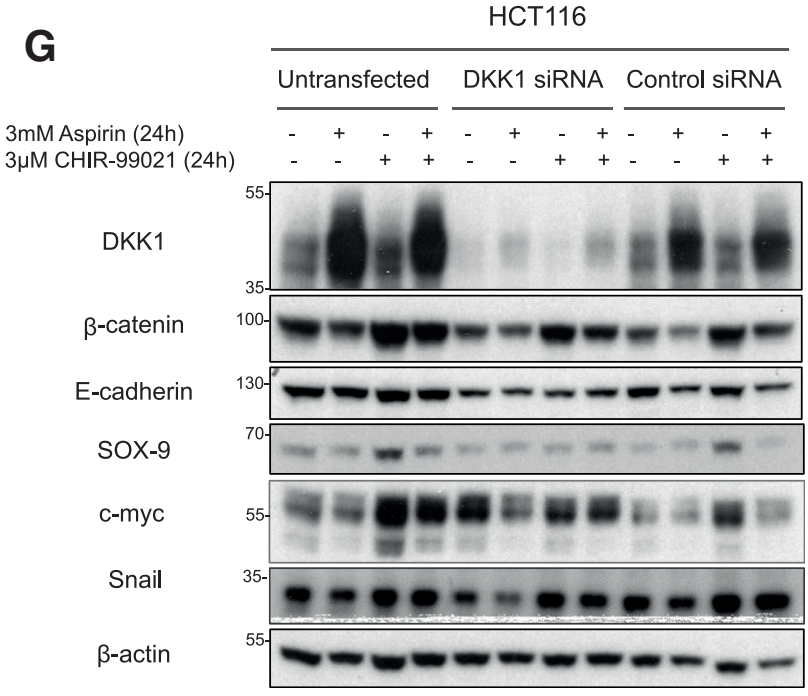
G
HCT116
Untransfected
DKK1 siRNA
Control siRNA
3mM Aspirin (24h)
3μM CHIR-99021 (24h)
DKK1
β-catenin
E-cadherin
SOX-9
c-myc
Snail
β-actin
55
35
100
130
70

(Oberkochen, Germany) microscope with a 4× objective. Quantification of wound closure was completed manually by measuring the wound area using Image J software (https://imagej.nih.gov/ij/) and comparing 48-hour image with the corresponding 0-hour image.

Single Cell Motility Assays

Cells were grown as a monolayer until approximately 40% confluence. Cell culture medium was replaced with medium containing either 0.5% or 10% fetal bovine serum and indicated compound treatments. Brightfield images were taken on a live cell imaging microscope, Zeiss Axiovert 200 microscope. A 10× objective was used with images captured every 30 minutes for 24 hours. Cell movement was analyzed, and distance was calculated using manual tracking and chemotaxis plugins for Image J software (https://imagej.nih.gov/ij/). Ten randomly selected cells were tracked for each well. Each experiment contained 2 technical replicates for each compound treatment, with 3 biological replicate experiments completed.

Organotypic Invasion Assays

Organotypic collagen-based invasion assays were performed as previously described.[67] To prepare 12 matrices, approximately 1×10^6 fibroblast cells were suspended in 3 mL of 10× minimum essential medium (Gibco, 11430030), which was then added to 25 mL of 2 mg/mL rat tail collagen that had been adjusted to pH 7.2 using 0.22 mol/L NaOH. The fibroblast-collagen mixture was plated into 12 × 35 mm plastic cell culture plates and allowed to set. Dulbecco modified Eagle medium containing 10% fetal bovine serum was added to each fibroblast-collagen matrix, and matrices were left to contract for 8 days, with medium replaced every second day. Fibroblast-collagen matrices were transferred to 24-well cell culture plates, and CRC cells were seeded on top of matrices in complete cell culture medium. Once cells were confluent, the fibroblast-collagen matrices were transferred to sterile stainless steel grids, which allowed the bottom of the matrices to be in contact with medium but not the CRC cells on top of the matrices. Compound treatments were added to the medium. Cells were left to invade matrices for 7 days before the fibroblast-collagen matrices were fixed in 4% paraformaldehyde (Thermo Scientific, 28908), paraffin-embedded, and sections stained with hematoxylin-eosin. Sections were imaged using a Zeiss Axioplan 2 microscope with 10× objective. Quantification of the number of invaded cells and the distance of invasion was performed manually using the Image J software (https://imagej.nih.gov/ij/). The percentage of invaded cells was normalized to the total cell number. Telomerase immortalized fibroblasts were used to create the fibroblast-collagen matrices and were provided by John Dawson (IGMM, Edinburgh).

Protein Extractions

Cells were washed and scraped in ice-cold PBS and then pelleted at 1800 rpm for 5 minutes. For whole cell protein extractions, cell pellets were resuspended in whole cell lysis buffer (20 mmol/L Tris-HCl [pH 7.5], 150 mmol/L NaCl, 1 mmol/L Na_2 EDTA, 1 mmol/L EGTA, 1% Triton, 2.5 mmol/L sodium pyrophosphate, 50 mmol/L sodium fluoride, 5 mmol/L beta-glycerophosphate, 50 nmol/L calyculin A, 1 mmol/L Na_3VO_4, 1× Roche complete EDTA-free protease inhibitor cocktail [Sigma-Aldrich, 1183617001], 1× Roche PhosSTOP [Sigma-Aldrich, 4906845001]) and incubated on ice for 30 minutes. Lysates were clarified at 13,000 rpm for 20 minutes. For cytoplasmic/nuclear protein extractions, cell pellets were resuspended in cytoplasmic lysis buffer (20 mmol/L Tris-HCl [pH 7.5], 0.1 mmol/L Na_2EDTA, 2 mmol/L $MgCl_2$, 2 μg/mL aprotinin, 2 μg/mL leupeptin, 0.3 μg/mL benzamidinchloride, 10 μg/mL trypsin inhibitor, 1% NP40, 50 nmol/L beta-2-mercaptoethanol, 1 mmol/L phenylmethylsulfonyl fluoride, 1× Roche complete EDTA-free protease inhibitor cocktail [Sigma-Aldrich, 1183617001], 1× Roche PhosSTOP [Sigma-Aldrich, 4906845001]) and incubated for 2 minutes at room temperature and then 10 minutes on ice. Cytoplasmic lysate was centrifuged at 3000 rpm for 5 minutes. The nuclear pellet was washed in detergent free cytoplasmic buffer 3 times. The residual pellet was resuspended in nuclear lysis buffer (20 mmol/L Hepes [pH 8], 0.4 mol/L NaCl, 25% glycerol, 1 mmol/L

Figure 11. (***See previous page***). **Aspirin treatment increases expression of intracellular DKK-1 while reducing secreted DKK-1.** (*A*) Immunoblotting for DKK-1 and LRP6 protein abundance in whole cell extracts and secreted DKK-1 protein abundance in media from HCT116 cells treated with 0.5 mmol/L aspirin, 3 mmol/L aspirin, 3 μmol/L CHIR-99021, or combination for 16 and 24 hours. (*B*) Immunoblotting for DKK-1 and LRP6 protein abundance in whole cell extracts and secreted DKK-1 protein abundance in media from Colo205 cells treated with 0.5 mmol/L aspirin, 3 mmol/L aspirin, 3 μmol/L CHIR-99021, or combination for 16 and 24 hours. (*C*) Immunoblotting of DKK-1, c-myc, and Snail protein abundance in cytoplasmic/nuclear extracts from HCT116 cells treated with 3 mmol/L aspirin for 24 hours. Immunoblotting data representative of 3 independent experiments. (*D*) DKK-1 transcript expression in organoids derived from human FAP normal colonic mucosa tissue and adenomatous tissue treated with 2 mmol/L aspirin for 4 hours. DKK-1 transcript levels are normalized to 18S transcripts, and data are expressed as fold-change compared with untreated control sample. DKK-1 transcript data represent 3 individual FAP patient samples. (*E*) DKK-1 transcript expression in fetal organoids treated with 2 mmol/L aspirin for 8 days. DKK-1 transcript levels are normalized to 18S transcripts, and data are expressed as fold-change compared with untreated control sample. (*F*) Average size of fetal organoids treated with 2 mmol/L aspirin for 8 days. Fetal organoid data represent 4 independent experiments. (G) Immunoblotting of DKK-1, β-catenin, E-cadherin, SOX-9, c-myc, and Snail protein abundance in untransfected HCT116 cells and HCT116 cells transfected with siRNA targeting DKK-1 or control siRNA. Cells were treated with 3 mmol/L aspirin, 3 μmol/L CHIR-99021, or combination for 24 hours. β-actin represents sample control. DKK-1 siRNA data representative of 3 independent experiments. Graphs represent individual data plots with overlay of mean and standard deviation. Statistical significance determined by Student *t* test. *Asterisks* denote *P* value (*<.05, **<.01, ***<.001, ****<.0001).

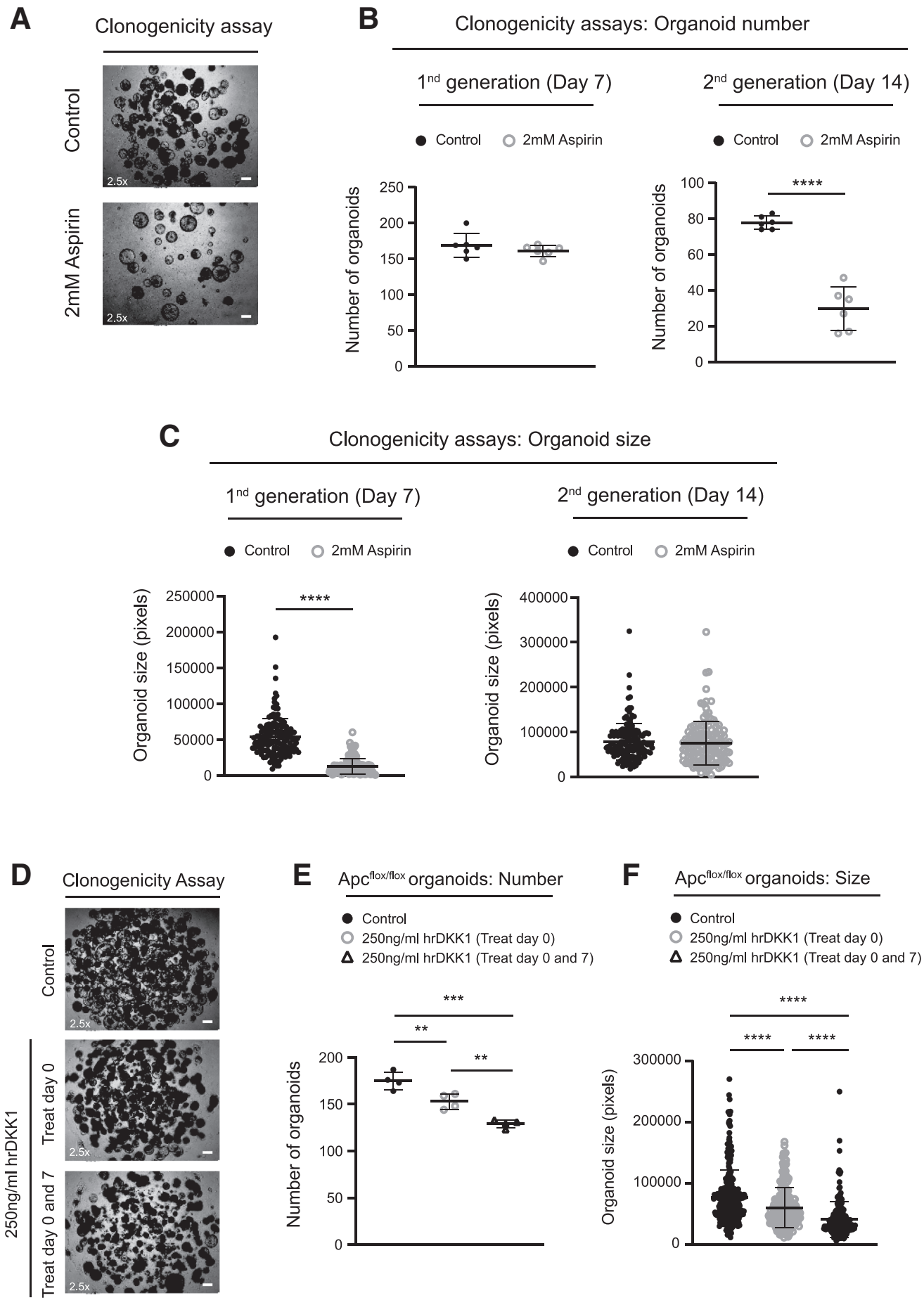
A
Clonogenicity assay
Control
2mM Aspirin
2.5x
B
Clonogenicity assays: Organoid number
1nd generation (Day 7)
2nd generation (Day 14)
Control
2mM Aspirin
Number of organoids
****
C
Clonogenicity assays: Organoid size
Organoid size (pixels)
D
Clonogenicity Assay
250ng/ml hrDKK1
Treat day 0
Treat day 0 and 7
E
Apcflox/flox organoids: Number
250ng/ml hrDKK1 (Treat day 0)
250ng/ml hrDKK1 (Treat day 0 and 7)
F
Apcflox/flox organoids: Size

Na_2EDTA, 0.5 mmol/L sodium fluoride, 0.5 mmol/L Na_3VO_4, 0.5 mmol/L dithiothreitol, 2 μg/mL aprotinin, 2 μg/mL leupeptin, 0.3 μg/mL benzamidinchloride, 1 μg/mL trypsin inhibitor, 1 mmol/L phenylmethylsulfonyl fluoride, 1× Roche complete EDTA-free protease inhibitor cocktail [Sigma-Aldrich, 1183617001], and 1× Roche PhosSTOP [Sigma-Aldrich, 4906845001]). The sample was frozen on dry ice, thawed, vortexed 3 times to disrupt nuclear membrane integrity, and then incubated on ice for 30 minutes. Nuclear lysate was clarified at 13,000 rpm for 20 minutes. Protein concentrations were measured using Pierce Coomassie Bradford protein assay kit (Thermo Scientific, 23200). Protein concentrations were adjusted to 1–3 μg/mL, and NuPAGE 4× LDS sample buffer (Thermo Scientific, NP0007) containing 10% beta-2-mercaptoethanol was added to samples. Samples were incubated at 95°C for 10 minutes before immunoblotting.

Immunoblotting

Proteins were separated by sodium dodecyl sulfate–polyacrylamide gel and transferred to polyvinylidene difluoride 0.2 μm transfer membrane (Thermo Scientific, 88520) using a Trans-blot SD semidry electrophoretic transfer cell (Bio-Rad, Hercules, CA; 1703940). Membranes were washed in PBS and blocked with 5% non-fat milk solution for 1 hour at room temperature. Membranes were washed in PBS containing 0.01% Tween20 and then incubated in primary antibody diluted in 5% bovine serum albumin solution containing 0.02% sodium azide for 16 hours at 4°C. Membranes were washed in PBS containing 0.01% Tween20 and then incubated with HRP-conjugated secondary antibody diluted in 5% non-fat milk solution containing 0.01% Tween20 for 1 hour at room temperature. After 3 × 10-minute washes in PBS containing 0.01% Tween20, antigen-antibody complexes were visualized by chemiluminescence using the Western blotting luminol reagent (Santa Cruz, sc-2048).

Immunoprecipitation

For immunoprecipitation, cells were lysed in an immunoprecipitation specific lysis buffer (40 mmol/L Hepes [pH 7.5], 150 mmol/L NaCl, 1 mmol/L Na_2EDTA, 10 mmol/L sodium pyrophosphate, 50 mmol/L glycerophosphate, 50 nmol/L sodium fluoride, 1 mmol/L Na_3VO_4, 1 mmol/L phenylmethylsulfonyl fluoride, 0.5% NP40, 1× Roche complete EDTA-free protease inhibitor cocktail [Sigma-Aldrich, 1183617001], 1× Roche PhosSTOP [Sigma-Aldrich, 4906845001]) for 45 minutes on ice before clarifying at 13,000 rpm for 20 minutes. Protein concentrations were determined as previously described. For each reaction 5 μL of anti-E-cadherin (BD Transduction Laboratories, 610181) or anti-β-catenin (BD Transduction Laboratories, 610153) antibody was added to 800 μg protein and incubated at 4°C for 24 hours. Dynabeads protein G (Thermo Scientific, 10003D) were equilibrated in immunoprecipitation lysis buffer, and then 50 μL was added to each reaction and incubated for 16 hours at 4°C. Beads were washed in PBS containing 0.02% Tween20 three times before elution by incubating beads in 100 μL NuPAGE 2× LDS sample buffer (Thermo Scientific, NP0007) containing 5% beta-2-mercaptoethanol at 70°C for 10 minutes. Samples were separated by sodium dodecyl sulfate–polyacrylamide gel as previously described.

Pull-down of Dickkopf-1 Protein From the Medium

Cells were treated with compounds as indicated. After treatment, the medium was collected from cells and incubated with StrataClean Resin (Agilent Technologies, Santa Clara, CA; 400714) in accordance with manufacturer's instructions. Briefly, 10 μL of StrataClean Resin was added to 1 mL supernatant and incubated on a rotating wheel for 1 hour at 4°C. The resin was pelleted, and supernatant was removed. The remaining resin was incubated in 50 μL NuPAGE 2× LDS sample buffer (Thermo Scientific, NP0007) containing 5% beta-2-mercaptoethanol at 70°C for 10 minutes. Samples were separated by sodium dodecyl sulfate–polyacrylamide gel, and DKK-1 protein was detected by immunoblotting using anti-DKK-1 antibody.

Immunofluorescence

Cells were seeded on glass coverslips and treated as indicated. Cells were fixed in 4% paraformaldehyde (Thermo Scientific, 28906) for 15 minutes, incubated in permeabilization buffer (0.2% Triton X) for 10 minutes, and then blocking buffer (3% goat serum, 3% bovine serum albumin) added for 1 hour, all at room temperature. E-cadherin (24E10) (Cell Signaling Technology, 3195), or

Figure 12. (***See previous page***). **Aspirin and DKK-1 treatment reduce number and size of $Apc^{flox/flox}$ organoids in clonogenicity assay.** (*A*) Brightfield images of organoids derived from $Apc^{flox/flox}$ mouse small intestine at day 14 of clonogenicity assay after treatment with 2 mmol/L aspirin. (*B*) Average number of organoids per well from clonogenicity assay at day 7 (first generation) and day 14 (second generation) after addition of 2 mmol/L aspirin on day 0. (*C*) Average size of organoids per well from clonogenicity assay at day 7 (first generation) and day 14 (second generation) after addition of 2 mmol/L aspirin on day 0. Aspirin clonogenicity assay data are representative of 6 technical replicates from organoids derived from 1 $Apc^{flox/flox}$ mouse tissue sample. (*D*) Brightfield images of $Apc^{flox/flox}$ organoids at day 14 of clonogenicity assay after addition of 250 ng/mL hrDKK1 as sole treatment on day 0 or double treatment on days 0 and 7. (*E*) Average number of organoids per well at day 14 of clonogenicity assay after addition of 250 ng/mL hrDKK1 as sole treatment on day 0 or double treatment on days 0 and 7. (*F*) Average size of organoids per well at day 14 of clonogenicity assay after addition of 250 ng/mL hrDKK1 as sole treatment on day 0 or double treatment on days 0 and 7. DKK-1 clonogenicity assay data represent 4 technical replicates from organoids derived from 1 $Apc^{flox/flox}$ mouse small intestine sample. Microscope objective magnification noted in *bottom left corner* of image. Scale bar = 300 μm. Graphs represent individual data plots with overlay of mean and standard deviation. Statistical significance determined by Student *t* test. *Asterisks* denote *P* value (*<.05, **<.01, ***<.001, ****<.0001).

ZO-1 (D6L1E) (Cell Signaling Technology, 13663), diluted 1:200, was incubated overnight at 4°C before incubation with goat anti-rabbit immunoglobulin G Alexa Fluor 488 antibody (Life Technologies, Carlsbad, CA; A32731) at 1:1000 for 1 hour at room temperature. For F-actin staining, after blocking cells were incubated with Alexa Fluor 488 phalloidin (Life Technologies, A12379) for 1 hour at room temperature. Coverslips were washed in PBS containing 0.01% Tween20 3 × 10 minutes before mounting. Cells were mouted with Vectashield mounting medium with DAPI (Vector Laboratories, H-1200-10). Cells were imaged on Zeiss Axioplan 2 using 10×, 40×, and 100× objectives maintaining consistent exposure settings for all treatment conditions. Quantification of immunofluorescence images was completed using Image J software (https://imagej.nih.gov/ij/). The mean grey area of each image was calculated and then divided by the number of nuclei per image to determine a value for staining intensity.

Quantitative Real-Time Polymerase Chain Reaction

After treatments, RNA was extracted using the Ribopure RNA isolation kit (Invitrogen, AM1924). RNA concentration was measured using a nanodrop and treated with RQ1 RNase-free DNAse (Promega, Madison, WI; M6101). cDNA synthesis was completed using M-MLV reverse transcriptase (Promega, M1701) and M-MLV reverse transcriptase buffer (Promega, M5313) following manufacturer's instructions. Quantitative real-time polymerase chain reaction was completed in triplicate in a 10 μL reaction with 2 μmol/L forward primer, 2 μmol/L reverse primer, 50% SYBR green master mix (Applied Biosystems, 4309155), and 2 μL cDNA (diluted 1:5) using a Lightcycler 480 (Roche). Primers used were as follows: *GAPDH* (F) [5′- GCACCGTCAAGGCTGAGAAC-3′], *GAPDH* (R) [5′-TGGTGAAGACGCCAGTGGA-3′]; *CDH1* (F) [5′-ATTCTGATTCTGCTGCTCTTG-3′], *CDH1* (R) [5′-AGTAGTCATAGTCCTGGTCTT-3′]; mouse *Lgr5* (F) [5′-GAGTCAACCCAAGCCTTAGTATCC-3′], mouse *Lgr5* (R) [5′-CATGGGACAAATGCAACTGAAG-3′]; human *Lgr5* (F) [5′-AATGGTGCCTCACAAATAAC-3′], human *Lgr5* (R) [5′-GAGATTAGGTAACTGATTGCAG-3′]; *18S* (F) [5′- GTAACCCGTTGAACCCCATT-3′], *18S* (R) [5′- CCATCCAATCGGTAGTAGCG-3′]; *TROY* (F) [5′-CTGGATTTGAAGTTTGTCTG-3′], *TROY* (R) [5′-CGTGTTTATTCCTGCTACTC-3′]; *Tcf7* (F) [5′-CACCACAGGAGGAAAAAGAAATG-3′], *Tcf7* (R) [5′-CAAGGAGGGCAACAGAAGATAC-3′]; *DKK-1* (F) [5′-GGTATTCCAGAAGAACCACCTTG-3′], and *DKK-1* (R) [5′-CTTGGACCAGAAGTGTCTAGCAC-3′]. The data were analyzed by using the comparative Ct method (ΔΔCt), with *GAPDH* or *18S* as the endogenous control gene.

Clonogenicity Assays

$Apc^{flox/flox}$ organoids were removed from Matrigel and incubated in trypsin for 20 minutes at 37°C to dissociate into single cells. Single cells in solution were passed through a 0.44-μm filter and manually counted using a Neubauer chamber. In each well of a 24-well plate, 1000 cells were plated in 10 μL BD Matrigel basement membrane matrix. After solidification of Matrigel, 500 μL mouse small intestine medium was added to each well, and treatment, 250 μg/mL human recombinant DKK-1 or 2 mmol/L aspirin, was added as indicated. Organoids were grown for 7 days and then imaged and manually counted. For a second generation, organoids were again removed from Matrigel, dissociated, counted, and replated as before. An additional treatment with 250 μg/mL human recombinant DKK1 was performed. Organoids were grown for another 7 days, imaged, and manually counted.

Transfection of Small Interfering RNAs

Cells were seeded into 6-well plates and grown to 70% confluence. Transfections were completed by using siRNAs that target human *DKK-1* (Dharmacon, Lafayette,CO; E-003843-00-0005) or nonspecific siRNA (Dharmacon, E-001910-01-5) as a negative control. For each well transfected, 25 nmol/L siRNA was diluted in 150 μL OptiMem (Gibco, 31985062). Separately, 10 μl Lipofectamine2000 (Invitrogen, 11668030) was diluted in 150 μL OptiMem (Gibco, 31985062). After incubating both reaction mixtures for 5 minutes at room temperature, they were combined and incubated for an additional 20 minutes at room temperature. The transfection mixture was added dropwise to the cells, and cells were cultured for an additional 24 hours before addition of compound treatments with aspirin and/or CHIR-99021 for 24 hours.

Statistics

All statistical tests and graphs were completed using Prism 8 (https://www.graphpad.com). Scatter plots show individual data points with an overlay of the mean and standard deviation. Statistical significance was determined by Student *t* test, with *P* value <.05 deemed significant. Asterisks denote the *P* value (*<.05, **<.01, ***<.001, ****<.0001).

References

1. Arnold M, Abnet CC, Neale RE, Vignat J, Giovannucci EL, McGlynn KA, Bray F. Global Burden of 5 major types of gastrointestinal cancer. Gastroenterology 2020;159:335–349.e15.
2. Rothwell PM. Aspirin in prevention of sporadic colorectal cancer: current clinical evidence and overall balance of risks and benefits. Recent Results Cancer Res 2012; 191:121–142.
3. Din FV, Theodoratou E, Farrington SM, Tenesa A, Barnetson RA, Cetnarskyj R, Stark L, Porteous ME, Campbell H, Dunlop MG. Effect of aspirin and NSAIDs on risk and survival from colorectal cancer. Gut 2010; 59:1670–1679.
4. Katona BW, Weiss JM. Chemoprevention of colorectal cancer. Gastroenterology 2020;158:368–388.

5. Clevers H, Nusse R. Wnt/beta-catenin signaling and disease. Cell 2012;149:1192–1205.
6. Reya T, Clevers H. Wnt signalling in stem cells and cancer. Nature 2005;434:843–850.
7. Snippert HJ, Schepers AG, van Es JH, Simons BD, Clevers H. Biased competition between Lgr5 intestinal stem cells driven by oncogenic mutation induces clonal expansion. EMBO Rep 2014;15:62–69.
8. Mani SA, Guo W, Liao MJ, Eaton EN, Ayyanan A, Zhou AY, Brooks M, Reinhard F, Zhang CC, Shipitsin M, Campbell LL, Polyak K, Brisken C, Yang J, Weinberg RA. The epithelial-mesenchymal transition generates cells with properties of stem cells. Cell 2008;133:704–715.
9. Dow Lukas E, O'Rourke Kevin P, Simon J, Tschaharganeh Darjus F, van Es Johan H, Clevers H, Lowe Scott W. Apc restoration promotes cellular differentiation and reestablishes crypt homeostasis in colorectal cancer. Cell 2015;161:1539–1552.
10. Yamamoto H, Sakane H, Yamamoto H, Michiue T, Kikuchi A. Wnt3a and Dkk1 regulate distinct internalization pathways of LRP6 to tune the activation of beta-catenin signaling. Dev Cell 2008;15:37–48.
11. Pinto D, Gregorieff A, Begthel H, Clevers H. Canonical Wnt signals are essential for homeostasis of the intestinal epithelium. Genes Dev 2003;17:1709–1713.
12. Kuhnert F, Davis CR, Wang HT, Chu P, Lee M, Yuan J, Nusse R, Kuo CJ. Essential requirement for Wnt signaling in proliferation of adult small intestine and colon revealed by adenoviral expression of Dickkopf-1. Proc Natl Acad Sci U S A 2004;101:266–271.
13. Niehrs C. Function and biological roles of the Dickkopf family of Wnt modulators. Oncogene 2006; 25:7469–7481.
14. Liu Z, Sun B, Qi L, Li Y, Zhao X, Zhang D, Zhang Y. Dickkopf-1 expression is down-regulated during the colorectal adenoma-carcinoma sequence and correlates with reduced microvessel density and VEGF expression. Histopathology 2015;67:158–166.
15. Pussila M, Sarantaus L, Dermadi Bebek D, Valo S, Reyhani N, Ollila S, Päivärinta E, Peltomäki P, Mutanen M, Nyström M. Cancer-predicting gene expression changes in colonic mucosa of Western diet fed Mlh1+/- mice. PLoS One 2013;8:e76865.
16. Cai Z, Cao Y, Luo Y, Hu H, Ling H. Signalling mechanism(s) of epithelial-mesenchymal transition and cancer stem cells in tumour therapeutic resistance. Clin Chim Acta 2018;483:156–163.
17. Vermeulen L, Snippert HJ. Stem cell dynamics in homeostasis and cancer of the intestine. Nature Reviews Cancer 2014;14:468–480.
18. Busch EL, McGraw KA, Sandler RS. The potential for markers of epithelial-mesenchymal transition to improve colorectal cancer outcomes: a systematic review. Cancer Epidemiol Biomarkers Prev 2014; 23:1164–1175.
19. Wang K, Song K, Ma Z, Yao Y, Liu C, Yang J, Xiao H, Zhang J, Zhang Y, Zhao W. Identification of EMT-related high-risk stage II colorectal cancer and characterisation of metastasis-related genes. Br J Cancer 2020; 123:410–417.
20. Kalluri R, Weinberg RA. The basics of epithelial-mesenchymal transition. J Clin Invest 2009; 119:1420–1428.
21. Chaffer CL, San Juan BP, Lim E, Weinberg RA. EMT, cell plasticity and metastasis. Cancer Metastasis Rev 2016; 35:645–654.
22. Jung Y-S, Park J-I. Wnt signaling in cancer: therapeutic targeting of Wnt signaling beyond β-catenin and the destruction complex. Exp Mol Med 2020;52:183–191.
23. Saito-Diaz K, Benchabane H, Tiwari A, Tian A, Li B, Thompson JJ, Hyde AS, Sawyer LM, Jodoin JN, Santos E, Lee LA, Coffey RJ, Beauchamp RD, Williams CS, Kenworthy AK, Robbins DJ, Ahmed Y, Lee E. APC inhibits ligand-independent Wnt signaling by the clathrin endocytic pathway. Dev Cell 2018; 44:566–581.e8.
24. Gala MK, Chan AT. Molecular pathways: aspirin and Wnt signaling—a molecularly targeted approach to cancer prevention and treatment. Clin Cancer Res 2015; 21:1543–1548.
25. Din FV, Valanciute A, Houde VP, Zibrova D, Green KA, Sakamoto K, Alessi DR, Dunlop MG. Aspirin inhibits mTOR signaling, activates AMP-activated protein kinase, and induces autophagy in colorectal cancer cells. Gastroenterology 2012;142:1504–1515 e3.
26. Moffat JG, Rudolph J, Bailey D. Phenotypic screening in cancer drug discovery: past, present and future. Nat Rev Drug Disc 2014;13:588–602.
27. Merenda A, Fenderico N, Maurice MM. Wnt signaling in 3D: recent advances in the applications of intestinal organoids. Trends Cell Biol 2020;30:60–73.
28. Sato T, Vries RG, Snippert HJ, van de Wetering M, Barker N, Stange DE, van Es JH, Abo A, Kujala P, Peters PJ, Clevers H. Single Lgr5 stem cells build crypt-villus structures in vitro without a mesenchymal niche. Nature 2009;459:262–265.
29. Sato T, Stange DE, Ferrante M, Vries RG, Van Es JH, Van den Brink S, Van Houdt WJ, Pronk A, Van Gorp J, Siersema PD, Clevers H. Long-term expansion of epithelial organoids from human colon, adenoma, adenocarcinoma, and Barrett's epithelium. Gastroenterology 2011;141:1762–1772.
30. Germann M, Xu H, Malaterre J, Sampurno S, Huyghe M, Cheasley D, Fre S, Ramsay RG. Tripartite interactions between Wnt signaling, Notch and Myb for stem/progenitor cell functions during intestinal tumorigenesis. Stem Cell Research 2014;13(Part A):355–366.
31. Michels BE, Mosa MH, Streibl BI, Zhan T, Menche C, Abou-El-Ardat K, Darvishi T, Czlonka E, Wagner S, Winter J, Medyouf H, Boutros M, Farin HF. Pooled in vitro and in vivo CRISPR-Cas9 screening identifies tumor suppressors in human colon organoids. Cell Stem Cell 2020;26:782–792 e7.
32. Thalheim T, Quaas M, Herberg M, Braumann U-D, Kerner C, Loeffler M, Aust G, Galle J. Linking stem cell function and growth pattern of intestinal organoids. Dev Biol 2018;433:254–261.
33. Sato T, Clevers H. Growing self-organizing mini-guts from a single intestinal stem cell: mechanism and applications. Science 2013;340:1190–1194.

34. Barker N, van Es JH, Kuipers J, Kujala P, van den Born M, Cozijnsen M, Haegebarth A, Korving J, Begthel H, Peters PJ, Clevers H. Identification of stem cells in small intestine and colon by marker gene Lgr5. Nature 2007;449:1003.
35. Farin HF, Van Es JH, Clevers H. Redundant sources of Wnt regulate intestinal stem cells and promote formation of Paneth cells. Gastroenterology 2012; 143:1518–1529.e7.
36. Brabletz T, Hlubek F, Spaderna S, Schmalhofer O, Hiendlmeyer E, Jung A, Kirchner T. Invasion and metastasis in colorectal cancer: epithelial-mesenchymal transition, mesenchymal-epithelial transition, stem cells and beta-catenin. Cells Tissues Organs 2005;179:56–65.
37. Rodrigues P, Macaya I, Bazzocco S, Mazzolini R, Andretta E, Dopeso H, Mateo-Lozano S, Bilić J, Cartón-García F, Nieto R, Suárez-López L, Afonso E, Landolfi S, Hernandez-Losa J, Kobayashi K, Ramón y, Cajal S, Tabernero J, Tebbutt NC, Mariadason JM, Schwartz S, Arango D. RHOA inactivation enhances Wnt signalling and promotes colorectal cancer. Nat Commun 2014; 5:5458.
38. Clayton NS, Ridley AJ. Targeting Rho GTPase signaling networks in cancer. Front Cell Dev Biol 2020;8.
39. Sousa-Squiavinato ACM, Rocha MR, Barcellos-de-Souza P, de Souza WF, Morgado-Diaz JA. Cofilin-1 signaling mediates epithelial-mesenchymal transition by promoting actin cytoskeleton reorganization and cell-cell adhesion regulation in colorectal cancer cells. Biochim Biophys Acta Molecular Cell Research 2019; 1866:418–429.
40. Huels DJ, Ridgway RA, Radulescu S, Leushacke M, Campbell AD, Biswas S, Leedham S, Serra S, Chetty R, Moreaux G, Parry L, Matthews J, Song F, Hedley A, Kalna G, Ceteci F, Reed KR, Meniel VS, Maguire A, Doyle B, Söderberg O, Barker N, Watson A, Larue L, Clarke AR, Sansom OJ. E-cadherin can limit the transforming properties of activating β-catenin mutations. Embo J 2015;34:2321–2333.
41. Semënov MV, Tamai K, Brott BK, Kühl M, Sokol S, He X. Head inducer Dickkopf-1 is a ligand for Wnt coreceptor LRP6. Curr Biol 2001;11:951–961.
42. Qi L, Sun B, Liu Z, Li H, Gao J, Leng X. Dickkopf-1 inhibits epithelial-mesenchymal transition of colon cancer cells and contributes to colon cancer suppression. Cancer Sci 2012;103:828–835.
43. Farin HF, Jordens I, Mosa MH, Basak O, Korving J, Tauriello DVF, de Punder K, Angers S, Peters PJ, Maurice MM, Clevers H. Visualization of a short-range Wnt gradient in the intestinal stem-cell niche. Nature 2016;530:340–343.
44. Keysselt K, Kreutzmann T, Rother K, Kerner C, Krohn K, Przybilla J, Buske P, Loffler-Wirth H, Loeffler M, Galle J, Aust G. Different in vivo and in vitro transformation of intestinal stem cells in mismatch repair deficiency. Oncogene 2017;36:2750–2761.
45. Xu F, Li S, Zhang J, Wang L, Wu X, Wang J, Huang Q, Lai M. Cancer stemness, immune cells, and epithelial-mesenchymal transition cooperatively predict prognosis in colorectal carcinoma. Clin Colorectal Cancer 2018; 17:e579–e592.
46. Wang W, Wan L, Wu S, Yang J, Zhou Y, Liu F, Wu Z, Cheng Y. Mesenchymal marker and LGR5 expression levels in circulating tumor cells correlate with colorectal cancer prognosis. Cell Oncol (Dordr) 2018;41:495–504.
47. Al-Kharusi MR, Smartt HJ, Greenhough A, Collard TJ, Emery ED, Williams AC, Paraskeva C. LGR5 promotes survival in human colorectal adenoma cells and is upregulated by PGE2: implications for targeting adenoma stem cells with NSAIDs. Carcinogenesis 2013; 34:1150–1157.
48. Feng Y, Sentani K, Wiese A, Sands E, Green M, Bommer GT, Cho KR, Fearon ER. Sox9 induction, ectopic Paneth cells, and mitotic spindle axis defects in mouse colon adenomatous epithelium arising from conditional biallelic Apc inactivation. Am J Pathol 2013; 183:493–503.
49. Zagorowicz E, Mroz A, Kraszewska E, Rupinski M, Kaminski MF, Regula J. Chronic low-dose aspirin use does not alter colonic mucosa in asymptomatic individuals: a prospective cross-sectional study (STROBE 1a). J Clin Pathol 2014;67:143–152.
50. Michels BE, Mosa MH, Grebbin BM, Yepes D, Darvishi T, Hausmann J, Urlaub H, Zeuzem S, Kvasnicka HM, Oellerich T, Farin HF. Human colon organoids reveal distinct physiologic and oncogenic Wnt responses. J Exp Med 2019;216:704–720.
51. Scheel C, Eaton EN, Li SH, Chaffer CL, Reinhardt F, Kah KJ, Bell G, Guo W, Rubin J, Richardson AL, Weinberg RA. Paracrine and autocrine signals induce and maintain mesenchymal and stem cell states in the breast. Cell 2011;145:926–940.
52. Khan P, Manna A, Saha S, Mohanty S, Mukherjee S, Mazumdar M, Guha D, Das T. Aspirin inhibits epithelial-to-mesenchymal transition and migration of oncogenic K-ras-expressing non-small cell lung carcinoma cells by down-regulating E-cadherin repressor Slug. BMC Cancer 2016;16:39.
53. Koontongkaew S, Monthanapisut P, Saensuk T. Inhibition of arachidonic acid metabolism decreases tumor cell invasion and matrix metalloproteinase expression. Prostaglandins Other Lipid Mediat 2010;93:100–108.
54. Guillem-Llobat P, Dovizio M, Bruno A, Ricciotti E, Cufino V, Sacco A, Grande R, Alberti S, Arena V, Cirillo M, Patrono C, FitzGerald GA, Steinhilber D, Sgambato A, Patrignani P. Aspirin prevents colorectal cancer metastasis in mice by splitting the crosstalk between platelets and tumor cells. Oncotarget 2016; 7:32462–32477.
55. Ying J, Zhou HY, Liu P, You Q, Kuang F, Shen YN, Hu ZQ. Aspirin inhibited the metastasis of colon cancer cells by inhibiting the expression of toll-like receptor 4. Cell Biosci 2018;8:1.
56. Drew DA, Cao Y, Chan AT. Aspirin and colorectal cancer: the promise of precision chemoprevention. Nat Rev Cancer 2016;16:173–186.
57. González-Sancho JM, Aguilera O, García JM, Pendás-Franco N, Peña C, Cal S, de Herreros AG, Bonilla F, Muñoz A. The Wnt antagonist DICKKOPF-1 gene is a

downstream target of β-catenin/TCF and is down-regulated in human colon cancer. Oncogene 2005; 24:1098–1103.
58. Aguilera O, Fraga MF, Ballestar E, Paz MF, Herranz M, Espada J, Garcia JM, Munoz A, Esteller M, Gonzalez-Sancho JM. Epigenetic inactivation of the Wnt antagonist DICKKOPF-1 (DKK-1) gene in human colorectal cancer. Oncogene 2006;25:4116–4121.
59. Koch S, Nava P, Addis C, Kim W, Denning TL, Li L, Parkos CA, Nusrat A. The Wnt antagonist Dkk1 regulates intestinal epithelial homeostasis and wound repair. Gastroenterology 2011;141:259–268, 68 e1–e8.
60. Gurluler E, Tumay LV, Guner OS, Kucukmetin NT, Hizli B, Zorluoglu A. The role of preoperative serum levels for Dickkopf-related protein 1 as a potential marker of tumor invasion in patients with stage II and III colon cancer. Eur Rev Med Pharmacol Sci 2014; 18:1742–1747.
61. Lattanzio S, Santilli F, Liani R, Vazzana N, Ueland T, Di Fulvio P, Formoso G, Consoli A, Aukrust P, Davi G. Circulating dickkopf-1 in diabetes mellitus: association with platelet activation and effects of improved metabolic control and low-dose aspirin. J Am Heart Assoc 2014;3: e001000.
62. Kim TH, Chang JS, Park KS, Park J, Kim N, Lee JI, Kong ID. Effects of exercise training on circulating levels of Dickkpof-1 and secreted frizzled-related protein-1 in breast cancer survivors: a pilot single-blind randomized controlled trial. PLoS One 2017;12: e0171771.
63. Bruschi M, Garnier L, Cleroux E, Giordano A, Dumas M, Bardet AF, Kergrohen T, Quesada S, Cesses P, Weber M, Gerbe F, Jay P. Loss of Apc rapidly impairs DNA methylation programs and cell fate decisions in Lgr5^{+} intestinal stem cells. Cancer Res 2020; 80:2101–2113.
64. Huang Z, Li S, Song W, Li X, Li Q, Zhang Z, Han Y, Zhang X, Miao S, Du R, Wang L. Lysine-specific demethylase 1 (LSD1/KDM1A) contributes to colorectal tumorigenesis via activation of the Wnt/beta-catenin pathway by down-regulating Dickkopf-1 (DKK1) [corrected]. PLoS One 2013;8:e70077.
65. Noreen F, Roosli M, Gaj P, Pietrzak J, Weis S, Urfer P, Regula J, Schar P, Truninger K. Modulation of age- and cancer-associated DNA methylation change in the healthy colon by aspirin and lifestyle. J Natl Cancer Inst 2014;106:dju161.
66. Bankhead P, Loughrey MB, Fernandez JA, Dombrowski Y, McArt DG, Dunne PD, McQuaid S, Gray RT, Murray LJ, Coleman HG, James JA, Salto-Tellez M, Hamilton PW. QuPath: open source software for digital pathology image analysis. Sci Rep 2017; 7:16878.
67. Timpson P, McGhee EJ, Erami Z, Nobis M, Quinn JA, Edward M, Anderson KI. Organotypic collagen I assay: a malleable platform to assess cell behaviour in a 3-dimensional context. J Vis Exp 2011:e3089.

Received July 15, 2020. Accepted September 18, 2020.

Correspondence
Address correspondence to: Farhat V. N. Din, MBChB, MD, Institute of Genetics and Molecular Medicine, University of Edinburgh, Western General Hospital, Crewe Road, Edinburgh, United Kingdom EH4 2XU. e-mail: Farhat.Din@igmm.ed.ac.uk; fax: 44-131-467-8450.

CRediT Authorship Contributions
Karen Dunbar, PhD (Data curation: Equal; Formal analysis: Lead; Investigation: Lead; Methodology: Lead; Writing – original draft: Equal; Writing – review & editing: Equal)

Asta Valanciute, PhD (Data curation: Equal; Formal analysis: Equal; Investigation: Equal; Methodology: Supporting; Supervision: Equal; Writing – original draft: Supporting; Writing – review & editing: Supporting)

Ana Cristina Silva Lima, BSc (Data curation: Supporting; Formal analysis: Supporting; Investigation: Supporting; Methodology: Supporting; Writing – review & editing: Supporting)

Paz Friele Vinuela, PhD (Data curation: Supporting; Formal analysis: Supporting; Investigation: Supporting; Methodology: Supporting)

Thomas Jamieson, PhD (Data curation: Supporting; Methodology: Supporting; Resources: Supporting)

Vidya Rajasekaran, PhD (Data curation: Supporting; Formal analysis: Supporting; Investigation: Supporting; Methodology: Supporting; Visualization: Supporting)

James Blackmur, MBChB (Data curation: Supporting; Methodology: Supporting)

Anna-Maria Ochocka-Fox, PhD (Data curation: Equal; Methodology: Supporting)

Alice Guazzelli, PhD (Data curation: Supporting)

Patrizia Cammareri, PhD (Methodology: Supporting; Supervision: Supporting; Writing – review & editing: Supporting)

Mark Arends, MBChB, MD (Supervision: Supporting)

Owen Sansom, PhD (Data curation: Supporting; Methodology: Supporting; Resources: Supporting; Writing – review & editing: Supporting)

Kevin B. Myant, PhD (Data curation: Supporting; Formal analysis: Supporting; Methodology: Supporting; Resources: Supporting; Supervision: Supporting; Writing – review & editing: Supporting)

Susan Farrington, PhD (Supervision: Supporting; Writing – review & editing: Supporting)

Malcolm G. Dunlop, MBChB, MD (Formal analysis: Supporting; Resources: Supporting; Supervision: Supporting; Writing – review & editing: Supporting)

Farhat Vanessa Nasim Din, MBChB, MD (Conceptualization: Lead; Formal analysis: Equal; Funding acquisition: Lead; Writing – original draft: Supporting; Writing – review & editing: Equal)

Conflicts of interest
The authors disclose no conflicts.

Funding
Supported by an MRC studentship to Karen Dunbar and clinical scientist fellowships to Farhat V. N. Din from Cancer Research UK (C26031/A11378) and the Chief Scientist Office, Scotland (SCAF/16/01). Further support was received from CRUK programme grant for VR (C348/A18927, PI MGD), CRUK Clinical Training Fellowship for JB (C157/A23218), and MRC Centre Grant - University Unit award for AMOF (U127527202, W. Bickmore PI, MGD - Project Leader).